General Disclaimer

One or more of the Following Statements may affect this Document

- This document has been reproduced from the best copy furnished by the organizational source. It is being released in the interest of making available as much information as possible.

- This document may contain data, which exceeds the sheet parameters. It was furnished in this condition by the organizational source and is the best copy available.

- This document may contain tone-on-tone or color graphs, charts and/or pictures, which have been reproduced in black and white.

- This document is paginated as submitted by the original source.

- Portions of this document are not fully legible due to the historical nature of some of the material. However, it is the best reproduction available from the original submission.

AgRISTARS

SM-G3-04400
TM-85006

A Joint Program for Agriculture and Resources Inventory Surveys Through Aerospace Remote Sensing

MARCH 1983

Soil Moisture

Technical Memorandum

CALCULATIONS OF RADAR BACKSCATTERING COEFFICIENT OF VEGETATION-COVERED SOILS

T. Mo, T.J. Schmugge and T.J. Jackson

CALCULATIONS OF RADAR BACKSCATTERING COEFFICIENT OF VEGETATION-COVERED SOILS

TSAN MO
COMPUTER SCIENCES CORPORATION
SILVER SPRING, MARYLAND 20910

THOMAS J. SCHMUGGE
HYDROLOGICAL SCIENCES BRANCH, CODE 924
NASA/GODDARD SPACE FLIGHT CENTER
GREENBELT, MARYLAND 20771

THOMAS J. JACKSON
USDA/ARS HYDROLOGY LABORATORY
BELTSVILLE, MARYLAND 20705

ABSTRACT

A model for simulating the measured radar backscattering coefficient of vegetation-covered soil surfaces is presented in this study. The model includes both coherent and incoherent components of the backscattered radar pulses from a rough soil surface. This surface is characterized by two parameters, the surface height standard deviation σ, and the horizontal correlation length ℓ. The effect of vegetation canopy scattering is also incorporated into the model by making the radar pulse subject to two-way attenuation and volume scattering when it passes through the vegetation layer. These processes are characterized by the two parameters, the canopy optical thickness τ and the volume scattering factor η. The model results agree well with the measured angular distributions of the radar backscattering coefficient for HH polarization at the 1.6 GHz and 4.75 GHz frequencies over grass-covered fields. These observations were made from an aircraft platform during 6 flights over a grass watershed in Oklahoma. It was found that the coherent scattering component is very important at angles near nadir, while the vegetation volume scattering is dominant at larger incident angles (> 30 degrees). The results show that least-squares fits to scatterometer data can provide reliable estimates of the surface roughness parameters, particularly the surface height standard deviation σ. The range of values for σ for the 6 flights is consistent with a 2 or 3 dB uncertainty in the magnitude of the radar response.

1. INTRODUCTION

Recently, there have been many microwave radar measurements made of Earth terrain under various surface conditions [1-8]. These measurements were usually taken with either truck-mounted or airborne scatterometers at various frequencies, and the resulting data are in the form of radar backscattering coefficients $\sigma^o(\theta)$, which are expressed in unit of decibels (dB) as a function of incidence angle θ. Analysis of the measured radar backscattering coefficients can provide valuable information about the surface soil moisture content, roughness parameters of the soil surface, and the vegetation cover. Theoretical simulations of the data can increase our understanding of the manner in which microwave radiation is backscattered from multilayer media (such as from vegetation-covered soils). Several theoretical models [9-14] have been developed to simulate the backscattering process, and they provide an excellent means of describing the returned radar signals to the scatterometers. However, the theoretical models are usually complicated and have many parameters, values of which are difficult, if not impossible, to obtain over large natural or agricultural fields. From an experimentalist's viewpoint, it would be desirable to have a simple model with a parametric description of the scattering media with the minimum number of parameters necessary to interpret the measured backscattering coefficients.

The present study was undertaken to develop a simple "user's" model for simulating the measured radar backscattering coefficients from vegetation-covered fields in conjunction with the data obtained by Jackson et al., [1, 2]. The model is based on the theoretical work by Fung and Eom [11], but modified to include the effect of a vegetation canopy. In addition, the Fresnel reflectivity which

appears in the model [11] was replaced by calculated soil surface reflectivity which was obtained from a radiative transfer model [15], using measured profiles of soil moisture and temperature. Coherent and incoherent scattering are included in the model in addition to the canopy volume scattering contributions. There are four parameters: two of these parameters specify the condition of the soil surface (the surface height standard deviation σ and the correlation length ℓ), and the other two define the characteristics of the canopy (the canopy optical thickness, τ, and the canopy volume scattering factor η).

Comparison of the model calculations with the measured radar backscattering coefficients at the frequencies 1.6 GHz (L-band) and 4.75 GHz (C-band) over grass-covered fields shows good agreement. The model calculations demonstrate that the large magnitudes of the measured $\sigma^o(\theta)$ at angles close to nadir are primarily due to the coherent scattering, and that the $\sigma^o(\theta)$ values at large incident angles ($\theta > 30^o$) can be attributed to vegetation canopy scattering. The incoherent scattering contributes to the backscattering coefficient at all angles for a rough soil surface.

2. THE MODEL

A radar pulse reflected from a vegetation-covered soil surface, is subject to two-way attenuation and scattering by the vegetation layer, as shown schematically in Figure 1. We assume that the geometrical configuration is symmetric with respect to the azimuth angle ϕ, and that Figure 1 corresponds to the $\phi = 0$ case. Backscattering occurs at $\theta_s = \theta$, $\phi_s = \pi$, and $\phi = 0$, where (θ, ϕ) denote the incident direction, and (θ_s, ϕ_s) the scattered direction.

The backscattering coefficient $\sigma^o(\theta)$ of vegetation-covered soils can be written in the form [8, 9],

$$\sigma^o(\theta) = \sigma_v^o(\theta) + \sigma_s^o(\theta)\ e^{-2\tau/\cos\theta} \qquad (1)$$

where $\sigma_v^o(\theta)$ is the vegetation backscattering coefficient, $\sigma_s^o(\theta)$ is the soil backscattering coefficient and τ is the optical thickness of the vegetation layer.

Following previous investigations [8, 9], the vegetation scattering component $\sigma_v^o(\theta)$ can be approximated by,

$$\sigma_v^o(\theta) = \frac{\eta \cos\theta}{2\tau}\ (1 - e^{-2\tau/\cos\theta}) \qquad (2)$$

where η, which depends on the canopy water content per unit area [8], is a vegetation volume scattering factor.

For a rough soil surface, the backscattering coefficient $\sigma_s^o(\theta)$ consists of two components: the coherent backscattering coefficient $\sigma_{coh}^o(\theta)$ and the incoherent backscattering coefficient $\sigma_{inc}^o(\theta)$. The coherent scattering component $\sigma_{coh}^o(\theta)$ occurs only in the specular direction (i.e., $\theta_s = \theta$), and

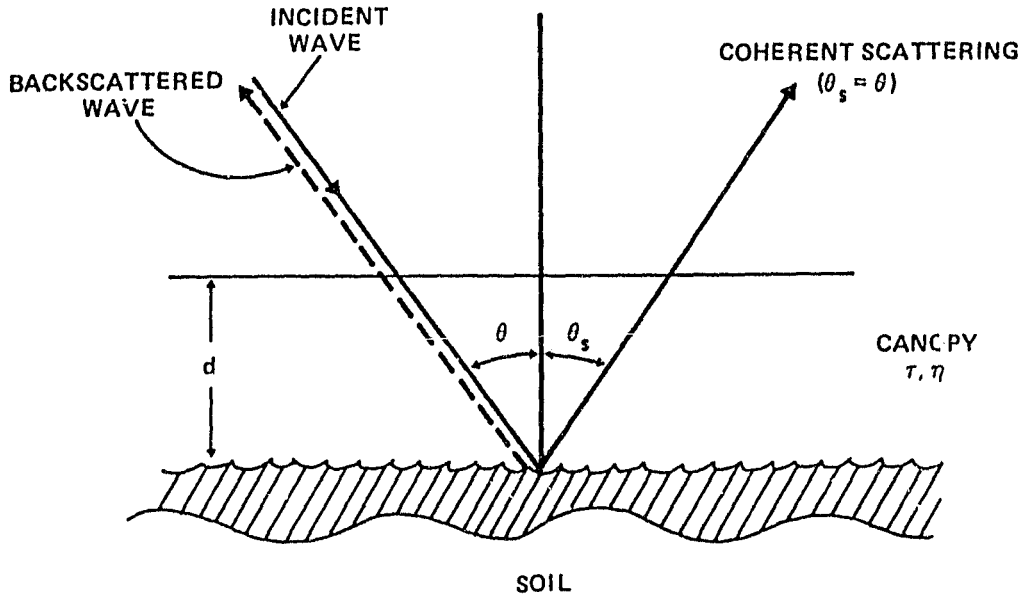

Figure 1. Schematic view of the scattering geometry. The θ and θ_s represent the incident and scattered angles, respectively. The thickness of the vegetation layer is denoted by d.

thus a monostatic radar would not receive any return power from the coherent scattering component except for normal incidence [14]. However, a radar with finite beamwidth antenna pattern can receive both coherent and incoherent scatterings, particularly near the nadir direction.

Thus, one can write the $\sigma_s^o(\theta)$ in the form,

$$\sigma_s^o(\theta) = \sigma_{coh}^o(\theta) + \sigma_{inc}^o(\theta) \tag{3}$$

The coherent scattering of microwave waves from a rough soil surface has been investigated by several authors [11, 17].

The general form, as a function of both incident and scattered angles, can be given by [11, 17],

$$\sigma_{coh}^o(\theta, \phi; \theta_s, \phi_s) = \pi k^2 |a_o|^2 \delta(q_x) \delta(q_y) e^{-q_z^2\sigma^2} \tag{4}$$

where k is the wave number of the incident wave, δ is the Dirac delta function and σ is the standard deviation of the surface height. The quantities q_x, q_y, q_z and a_o are defined as [11, 14],

$$\begin{aligned} q_x &= k(\sin\theta_s \cos\phi_s - \sin\theta \cos\phi) \\ q_y &= k(\sin\theta_s \sin\phi_s - \sin\theta \sin\phi) \\ q_z &= k(\cos\theta_s \mp \cos\theta) \\ a_o &= |R_{pp}| (\cos\theta + \cos\theta_s) \cos(\phi_s - \phi), \quad (pp = HH \text{ or } VV) \end{aligned} \tag{5}$$

The delta functions in Equation (4) limit the coherent scattering to the specular direction, $\theta_s = \theta$ and $\phi_s = \phi$. The magnitude of this coherent scattering along the specular direction can be obtained by integrating Equation (4) across

the $\theta_s = \theta$ and $\phi_s = \phi$ direction of the scattered solid angle $d\Omega_s = d\cos\theta_s d\phi_s$, and the result is approximated by $\sigma^o_{coh}(\theta)$, i.e.,

$$\sigma^o_{coh}(\theta) = \int_{\Delta\Omega_s} \sigma^o_{coh}(\theta,\phi;\theta_s,\phi_s)\, d\Omega_s \qquad (6)$$

$$= 4\pi\, |R_{pp}|^2 \cos\theta\, e^{-h\cos^2\theta}$$

where $h = 4k^2\sigma^2$, and the quantity $|R_{pp}|^2$ represents the reflectivity of a smooth surface.

The coherent backscattering coefficient $\sigma^o_{coh}(\theta)$ defined in Equation (6) corresponds to a monochromatic radar beam. In practice, a radar has a transmitting antenna pattern with a finite beamwidth, and thus the actual coherent backscattering coefficient is distributed according to the transmitting antenna pattern $G_t(\theta)$. Also the received radar power is determined by the receiving antenna pattern $G_r(\theta')$ for a returned coherent beam located at an angle θ', measured from the center of the antenna beam.

Assume that the product of the antenna gain patterns is represented by the Gaussian form,

$$f(\theta) = G_t(\theta)\, G_r(\theta) = \exp\left[-\frac{a(\theta - \theta_o)^2}{\beta^2}\right] \qquad (7)$$

where β is the 3-dB antenna beamwidth and $a = 4\ \ell n 2$. The angle θ_o is the location of the center of the antenna beam.

Since coherent scattering occurs only in the specular direction (see Figure 1), the functional form of receiving antenna gain pattern for coherent scattering can be obtained

from the one given in Equation (7) by changing $(\theta - \theta_o)$ to $(\theta + \theta_o)$. The returned coherent scattering at an angle $\theta' = \theta + \theta_o$ can make contributions to the measured backscattering coefficient through an appropriate 'coherent' antenna gain pattern, which can be approximated by,

$$g_c(\theta) = G_t(\theta)\, G_r(\theta') = \exp\left[-\frac{a(\theta - \theta_o)^2}{2\beta^2}\right]\exp\left[-\frac{a(\theta + \theta_o)^2}{2\beta^2}\right]$$

$$= \exp\left[-\frac{a(\theta^2 + \theta_o^2)}{\beta^2}\right] \qquad (8)$$

Therefore, the 'measureable' coherent contribution to the backscattering coefficient can be defined by the weighted quantity,

$$\langle \sigma^o_{coh}(\theta) \rangle = g_c(\theta)\ \sigma^o_{coh}(\theta) \qquad (9)$$

where $\sigma^o_{coh}(\theta)$ and $g_c(\theta)$ are given by Equations (6) and (8), respectively.

The incoherent backscattering coefficient $\sigma^o_{inc}(\theta)$ in Equation (3) depends on the statistical properties of a rough surface: the surface height standard deviation σ and the correlation length ℓ. The latter provides a reference for estimating the statistical independence of two points on a surface [14]. Models for $\sigma^o_{inc}(\theta)$ have been developed by many authors [11, 14, 16, 17]. The one developed by Fung and Eom [11] is relatively simple in application and it will be further developed in this study to fit the backscattering coefficient data.

Backscattering coefficient from a rough soil surface depends on the surface correlation function of its height distribution. Both Gaussian and non-Gaussian correlation functions have been used for numerical calculations of backscattering coefficient [11, 14, 23]. For mathematical simplicity, the Gaussian form of correlation function has been widely used in the computation of backscattering coefficient. In this study, we assume that a rough soil surface has a Gaussian surface correlation function $\rho(\xi)$ and a horizontal correlation length ℓ, i.e.,

$$\rho(\xi) = \exp(-\xi^2/\ell^2) \tag{10}$$

where ξ is a distance between two points on the horizontal surface. Then following a similar process as given in reference [16], one can show that the incoherent backscattering coefficient $\sigma^o_{inc}(\theta)$ for pp polarization is given by the form [11, 14],

$$\sigma^o_{inc}(\theta) = (k\ell)^2 \left[|R_{pp}|^2 (1 + \sin^2\theta) + \mathrm{Re}(R_{pp}R^*_{ppl}) \sin 2\theta \right] \times e^{-h\cos^2\theta} \sum_{n=1}^{\infty} \frac{(h\cos^2\theta)^n}{n!n} \exp\left[-\frac{(k\ell \sin\theta)^2}{n} \right] \tag{11}$$

where $h = 4k^2\sigma^2$, $|R_{pp}|^2$ denotes the smooth surface reflectivity, and R^*_{ppl} is the complex conjugate of R_{ppl}, which is a component of the reflectivity. For pp = HH, it can be related to R_{HH} by the relation [11, 14],

$$R_{HHl} = -R_{HH} \frac{2 \sin\theta}{\cos\theta + \sqrt{\varepsilon_s - \sin^2\theta}} \tag{12}$$

where ϵ_s is the complex dielectric constant of soil. For other polarizations, explicit forms of R_{ppl} can be found in references [11, 14].

In applying Equation (11) to the backscattering coefficient, the quantity $\sigma^o_{inc}(\theta)$ should be weighted by the antenna gain pattern $f(\theta)$ given in Equation (7). Similar to $<\sigma^o_{coh}(\theta)>$ in Equation (9), one can define the quantity,

$$<\sigma^o_{inc}(\theta)> = f(\theta)\ \sigma^o_{inc}(\theta) \tag{13}$$

as the weighted incoherent backscattering coefficient.

Therefore, the total soil backscattering coefficient, $<\sigma^o_s(\theta)>$ weighted by appropriate antenna gain patterns, can be written in the form,

$$\begin{aligned} <\sigma^o_s(\theta)> &\equiv <\sigma^o_{coh}(\theta)> + <\sigma^o_{inc}(\theta)> \\ &= g_c(\theta)\sigma^o_{coh}(\theta) + f(\theta)\ \sigma^o_{inc}(\theta) \\ &= f(\theta)\left[\ \sigma^o_{coh}(\theta)\ \exp\left(-\frac{2a\theta\theta_o}{\beta^2}\right) + \sigma^o_{inc}(\theta)\right] \end{aligned} \tag{14}$$

where Equations (7) and (8) have been employed in arriving at the last step in Equation (14).

For comparing with the data, the calculated backscattering coefficient $<\sigma^o_s(\theta)>$ from Equation (14) and the vegetation backscattering coefficient $\sigma^o_v(\theta)$ from Equation (2) should be averaged over the main beam of the antenna patterns, or more precisely, over the illuminated target area bounded by the main antenna beam. Allen et al., [7] have presented the detailed description of the geometrical configuration, and

our final result of the weighted average total backscattering coefficient $\langle\sigma^o(\theta)\rangle_{ave}$ can be written as,

$$\langle\sigma^o(\theta)\rangle_{ave} = \frac{1}{A}\int f(\theta)\left[\sigma^o_{coh}(\theta)\,\exp\left(-\frac{2a\theta\theta_o}{\beta^2}\right) + \sigma^o_{inc}(\theta) + \sigma^o_v(\theta)\right]\tan\theta\,d\theta \tag{15}$$

where the factor $\tan\theta$ comes from the geometrical configuration of the illuminated target area [7], and the normalization factor A is given by:

$$A = \int f(\theta)\,\tan\theta\,d\theta \tag{16}$$

Equation (15) will be used to fit the data, as described in the next section.

3. THE RESULTS

The formulas derived in the previous section were used to fit the measured backscattering coefficient [1,2] at L and C-band frequencies over 4 different grass-covered watersheds located near Chickasha, Oklahoma in 1978 and 1980. The data for HH polarization, taken with airborne scatterometers from an altitude of 300 meter, were given in decibels (dB) at incident angles between 5° and 50° at 5° increments. The soil texture of the fields is silt loams [18] consisting of 33% sand, 20% clay, and 45% silt, approximately. Soil moisture profiles were measured within three depth intervals: 0-2.5 cm, 2.5-5 cm, and 5-15 cm. Also measured were the soil temperatures. These measured soil moistures and temperatures were employed to calculate the soil dielectric constant ε_s and the soil surface reflectivity $|R_{pp}|^2$, using Wilheit's radiative transfer model [15]. These calculated reflectivity values were used to fit the data, although there would be no significant difference obtained if the Fresnel reflectivity was employed.

Equation (15) was used to fit (by a least-squares criterion) the measured backscattering coefficient as a function of incident angle θ. There are four adjustable parameters: σ, ℓ, τ, and η. The first two (i.e., the surface height standard deviation σ and the correlation length ℓ) specify in a statistical manner the geometrical conditions of the soil surface, while the last two (the canopy optical thickness τ and the canopy scattering factor η) describe the characteristics of the vegetation canopy, which is assumed to form a uniform layer over a soil surface.

In applying Equation (15) to fit the data, one needs to know the 3-dB beamwidth of the antenna pattern. According to Wang [19], the L-band scatterometer had $\beta \simeq 9^{\circ}$, and the β value for C-band was approximately $\beta \simeq 2.5^{\circ}$ [20].

Theoretically, any one of the four parameters can be varied to obtain the best fit to the data. However, best fit results show the vegetation backscattering coefficient $\sigma_v^o(\theta)$ is relatively small (although it dominates at angles greater 30^o), and that one can keep τ at a fixed value in fitting the data. This is due to the fact that the τ value for a grass canopy is usually very small and therefore Equation (2) essentially reduces to the form $\sigma_v^o(\theta) \simeq \eta(1 - \tau/\cos\theta)$. Thus good fits to the data can be obtained by varying η, keeping τ fixed.

A previous investigation [21] shows that τ is proportional to the vegetation canopy water content W (in kg/m^2), and that it can be given by the simple form,

$$\tau = cW \tag{17}$$

where c is a frequency dependent proportionally constant.

For L-band, it has been shown that $c \simeq 0.12$ [21]. The τ values for C-band are 2 to 5 times larger than those for L-band. In the present work, the L-band data were fitted by keeping $\tau = 0.06$, which corresponds to an assumption of canopy water content $W = 0.5\ kg/m^2$, a typical value for 10-30cm tall grass [22]. For C-band, it was assumed that $\tau = 0.12$ for all the cases considered.

With τ fixed at the above values, there are only the three parameters σ, ℓ, and η to be varied to fit the data. Since the wave number k always appears in places where σ or ℓ occurs in the formulas (see Equations 6 and 11), it is convenient to take the dimensionless quantities $k\sigma$ and $k\ell$, instead of σ and ℓ, as the adjustable parameters.

Comparisons of some typical best fits (at L- and C-bands) to the data are shown in Figures 2 to 5 for the four different grass fields. In these figures, the solid curves represent

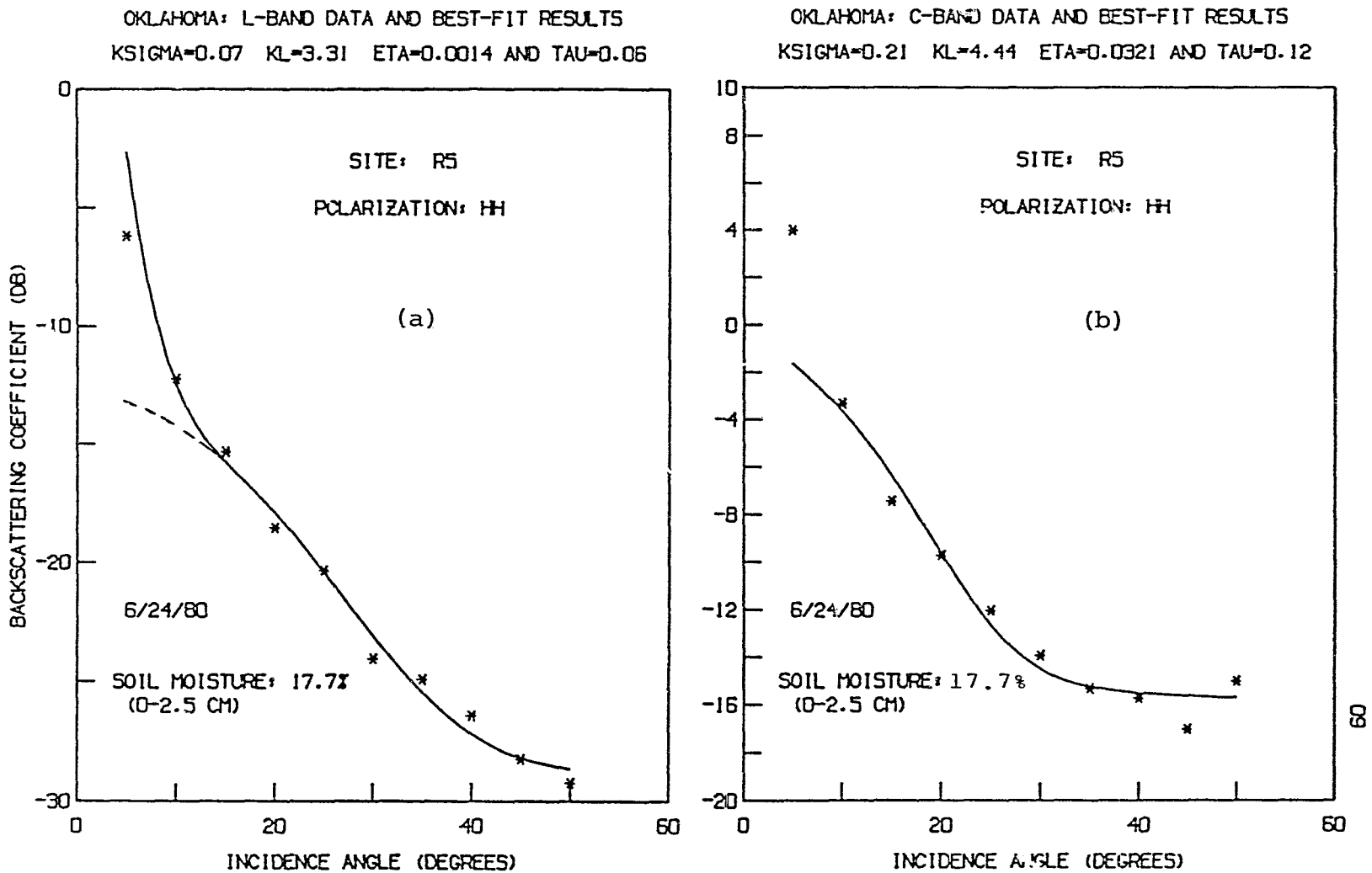

Figure 2. Comparison of calculated and measured backscattering coefficients. The asterisks denote the scatterometer data over site R5, and the solid curves represent the calculations obtained with parameters listed at the tops. The dashed curve (at the L-band) would result if the coherent scattering was excluded from the calculation.

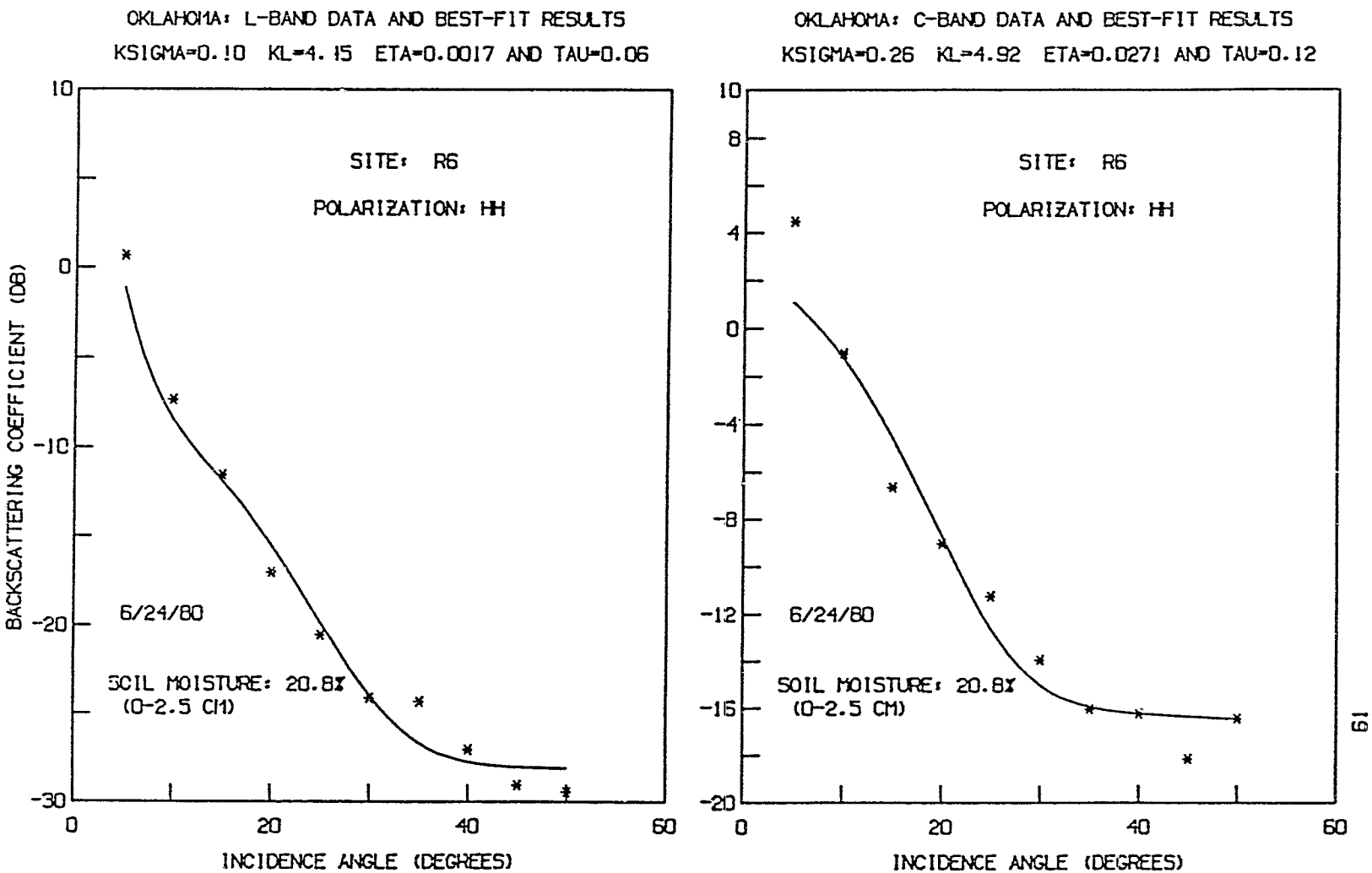

Figure 3. Comparison of calculations (solid curves) and scatterometer data (asterisks) taken at L- and C-bands over site R6

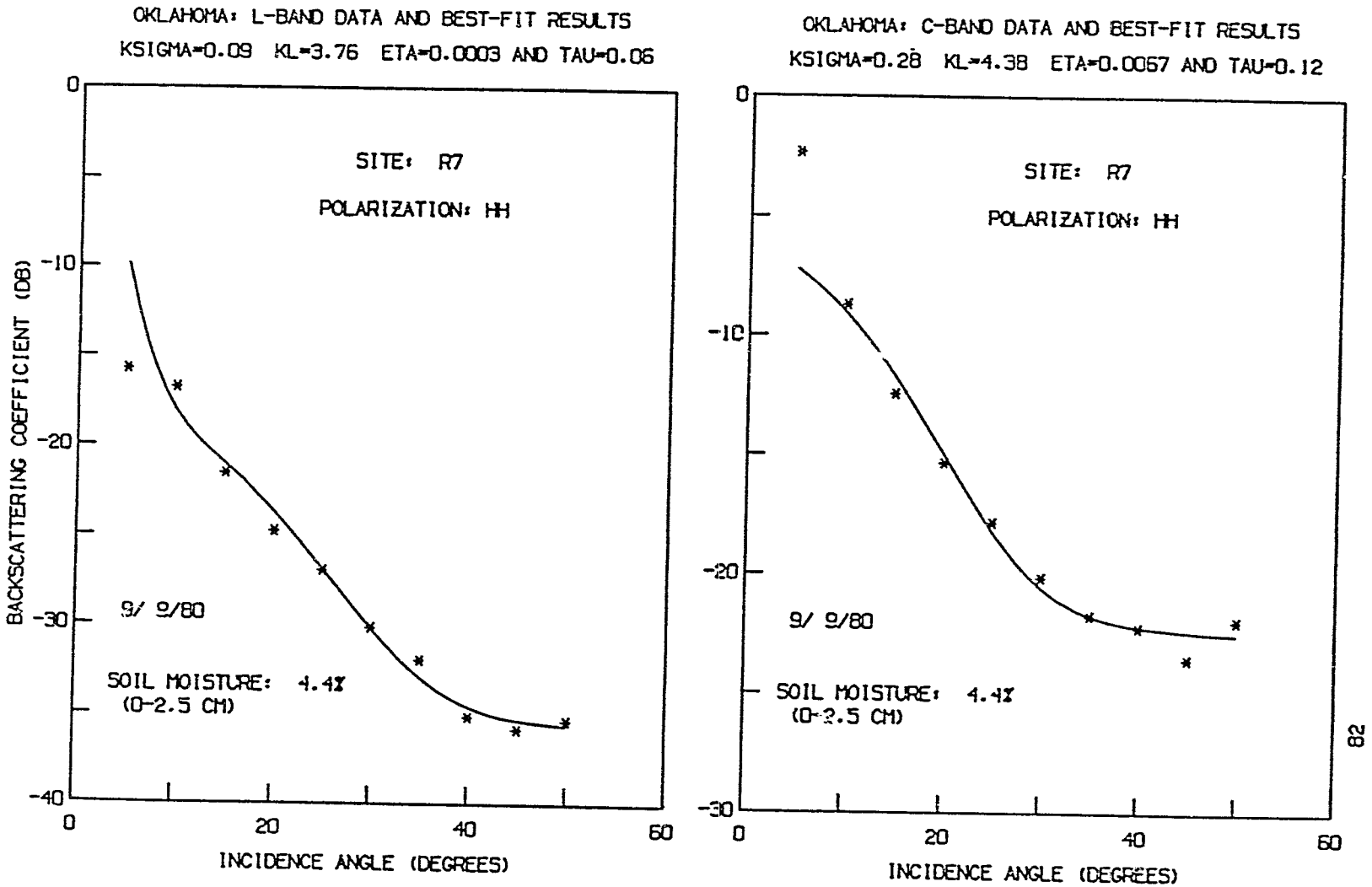

Figure 4. Comparison of calculations (solid curves) and scatterometer data (asterisks) taken at L- and C-bands over site R7.

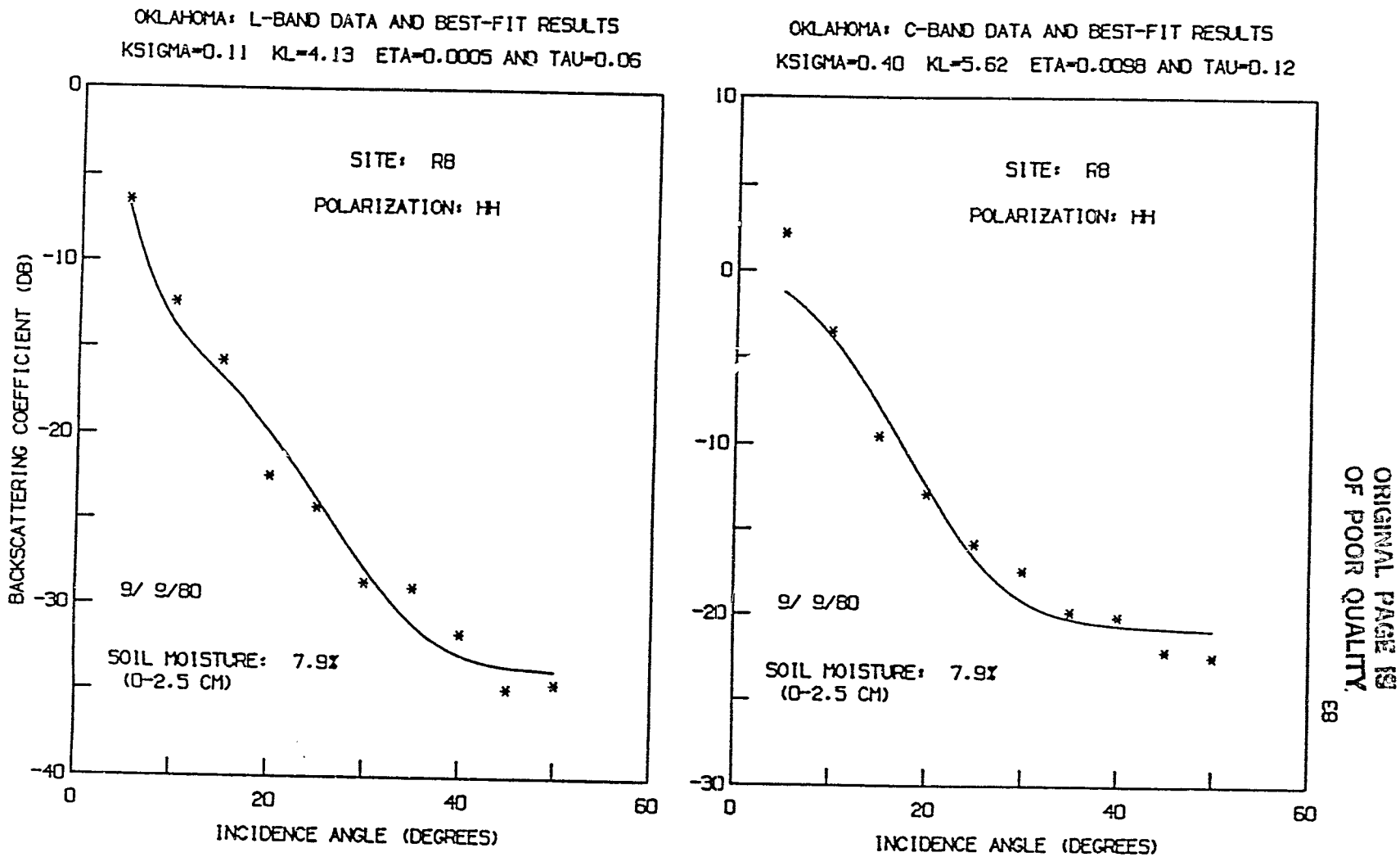

Figure 5. Comparison of calculations (solid curves) and scatterometer data taken at L- and C-bands over site R8.

the calculated backscattering coefficients (in dB) for the HH polarization, and the asterisks denote the data. The parameter values used in the calculations are listed at the top of each figure, and the soil moisture content (in wt-%) of the 0-2.5 cm surface layer is indicated on the lower part of each figure, together with the date (month/day/year) of the scatterometer measurement.

Figure 2 displays the results for the site R5, which was well managed pasture land [1]. The L-band results are shown in part (a), while those for C-band are given in part (b). The model calculations (the solid curves) in Figure 2 agree well with the observations at all incidence angles, except at 5^{o}, where the scatterometer data probably contain large uncertainties due to instrumental system problems at such near nadir angles [20].

The dashed curve in Figure 2a resulted from excluding the coherent backscattering component $\sigma^{o}_{coh}(\theta)$. This shows that the coherent scattering makes large contribution at angles near nadir, and its importance can be ignored when the incidence angle is greater than 15^{o}.

The $k\sigma$ value used in obtaining the L-band result as shown in Figure 2a is smaller than that of C-band (Figure 2b) by a factor 3, which is the correct ratio of the k values of C-band to L-band if σ remains constant, as expected. On the other hand, the ratio of the two $k\ell$ values in Figures 2a and 2b does not maintain this 1:3 relationship, thus it implies that the correlation length ℓ, which best describes the surface backscatter is still wavelength dependent. This indicates that, perhaps, additional parameters are required to specify the soil surface conditions [7, 11].

Figure 3 shows the results for site R6, which was nearly identical to R5 in terms of soil condition and vegetation cover. The best-fit parameter values listed in Figure 3 are

comparable to those in Figure 2, as expected for two nearly identical fields.

Figures 4 and 5 demonstrate the best-fit results and the observations over the two watersheds R7 and R8, which were poorly managed pastures [1,2]. Hydrologically, sites R7 and R8 were considered identical. The soils (as shown by the soil moistures in Figures 4 and 5) in both sites were very dry on the experiment date (September 9, 1980). The calculated results as shown by the solid curves in Figures 4 and 5 agree well with the observations, both in magnitude and angular variations. Also, the best-fit $k\sigma$ values (as listed at the top of Figures 4 and 5) vary with frequency as expected.

Additional calculations and comparisons with the data are given in Appendix A. The parameter values used in the calculations of Figures 2 to 4, and those of Appendix A are given in Table 1, for both L- and C-bands. The last column of Table 1 also lists the soil moisture content (in weight-percent, or wt-%) within the 0-2.5 cm surface layer of soil. The average value of the parameters are listed in the bottom row in Table 1.

Table 1 shows that the surface parameters for sites R5 and R6 have approximately the same numerical values, and that those for R7 and R8 are also similar. Generally, the $k\sigma$ values for R7 and R8 are larger than those of R5 and R6. This is in agreement with the fact that the soil surfaces of sites R7 and R8 were more highly eroded and therefore were rougher than those of R5 and R6 [1, 2].

Table 1. Best-fit parameters obtained from fits to the scatterometer data. Note that the value of $\tau = 0.06$ is fixed for L-band and $\tau = 0.12$ for C-band. The last column gives the soil moisture (SM) within the 0-2.5 cm surface layer. The average values of these parameters are listed in the bottom row.

DATE	SITE	L-BAND				C-BAND				SM (0–2.5cm) (WT–%)
		$k\sigma$	$k\ell$	η	τ	$k\sigma$	$k\ell$	η	τ	
5/01/78	R5	0.09	2.86	2.3×10^{-3}	0.06	–	–	–	–	21.2
5/12/78		0.14	4.62	3.0×10^{-3}	0.06	0.11	4.73	1.6×10^{-2}	0.12	16.2
5/30/78		0.11	4.40	3.6×10^{-3}	0.06	0.24	5.31	2.8×10^{-2}	0.12	30.1
6/24/80		0.07	3.31	1.4×10^{-3}	0.06	0.21	4.44	3.2×10^{-2}	0.12	17.7
8/14/80		0.08	3.68	0.2×10^{-3}	0.06	0.22	3.74	0.8×10^{-2}	0.12	2.9
9/09/80		0.05	3.24	0.4×10^{-3}	0.06	0.16	4.20	1.0×10^{-2}	0.12	7.9
5/01/78	R6	0.12	4.76	6.7×10^{-3}	0.06	–	–	–	–	22.0
5/12/78		0.22	5.03	2.6×10^{-3}	0.06	0.14	4.89	1.6×10^{-2}	0.12	15.6
5/30/78		0.10	4.15	5.2×10^{-3}	0.06	0.25	4.74	3.1×10^{-2}	0.12	28.4
6/24/80		0.10	4.45	1.7×10^{-3}	0.06	0.26	4.92	2.7×10^{-2}	0.12	20.8
8/14/80		0.13	4.68	0.4×10^{-3}	0.06	0.34	5.14	0.9×10^{-2}	0.12	1.9
9/09/80		0.06	3.90	0.3×10^{-3}	0.06	0.20	4.99	1.0×10^{-2}	0.12	5.6
5/01/78	R7	0.19	3.80	6.1×10^{-3}	0.06	–	–	–	–	19.6
5/12/78		0.14	3.36	4.0×10^{-3}	0.06	0.21	3.05	1.0×10^{-2}	0.12	12.7
5/30/78		0.22	4.67	11.0×10^{-3}	0.06	0.49	5.97	3.8×10^{-2}	0.12	19.9
6/24/80		0.16	3.91	1.6×10^{-3}	0.06	0.40	5.65	2.6×10^{-2}	0.12	15.4
8/14/80		0.16	4.22	0.7×10^{-3}	0.06	0.38	4.71	0.9×10^{-2}	0.12	1.4
9/09/80		0.09	3.76	0.3×10^{-3}	0.06	0.28	4.38	0.7×10^{-3}	0.12	4.4
5/01/78	R8	0.16	3.20	14.3×10^{-3}	0.06	–	–	–	–	22.3
5/12/78		0.14	3.98	8.9×10^{-3}	0.06	0.15	4.20	2.4×10^{-2}	0.12	13.0
5/30/78		0.21	4.79	16.9×10^{-3}	0.06	0.36	5.07	4.4×10^{-2}	0.12	23.5
6/24/80		0.42	6.92	3.1×10^{-3}	0.06	0.45	6.05	3.9×10^{-2}	0.12	16.2
8/14/80		0.17	3.70	1.2×10^{-3}	0.06	0.54	5.06	1.1×10^{-2}	0.12	2.2
9/09/80		0.11	4.13	0.5×10^{-3}	0.06	0.40	5.62	1.0×10^{-2}	0.12	7.9
AVERAGE:		0.14	4.15	4.0×10^{-3}	0.06	0.29	4.84	2.1×10^{-2}	0.12	

9164/83

4. DISCUSSION

The surface parameter values (for the same site) given in Table 1 show some variations from one day to another in the same year. It is possible that this is due to the fact the surface conditions changed during the period of data acquisition. However, another possible explanation is that the apparent variation in the best fit parameters might be due to small errors in absolute calibration of the scatterometer system from one flight to another.

To investigate this possibility, we made some studies of the backscattering coefficient sensitivity to the parameters for L-band. The results are given in Table 2, which lists the best-fit parameters values that would result, if the measured backscattering coefficients, $\sigma^{o}(\theta)$, were arbitrarily increased by 2 dB and 5 dB, respectively, at all angles.

Comparison of results in Tables 1 and 2 reveals that in the case of $\sigma^{o}(\theta)$ + 5dB, the $k\sigma$ values (in Table 2) are approximately 2 times larger than the corresponding ones in Table 1, and that the $\sigma^{o}(\theta)$ + 2dB case requires about a 50% increment in the surface parameter values. Therefore, if the soil surface conditions of the sites remained the same during the data taking period, particularly for the same year, the apparent variations in the best-fit parameter value (in Table 1) can be attributed to small errors of the scatterometer system from one flight to the other. Also an assumption of ± 2 dB errors in the measured angular distributions of the backscattering coefficient would adequately account for the range of variation in the parameter values as given in Table 1. The η values (C-band) in Table 1 are comparable to results reported by other investigators [8] at the 8.6 GHz frequency for a wheat field, which is assumed to be structurally similar to the grass in the pasture.

Table 2. Best-fit parameters (L-band) obtained from fits the cases of $\sigma^o(\theta)$ + 2 dB, and $\sigma^o(\theta)$+ 5 dB, respectively, as explained in the text. Note that τ = 0.06 was used in all cases.

DATE	SITE	$\sigma^o(\theta)$ + 2 db				$\sigma^o(\theta)$ + 5 db				SM (0–2.5cm) (WT %)
		$k\sigma$	$k\ell$	η	τ	$k\sigma$	$k\ell$	η	τ	
5/01/78	R5	0.11	3.48	5.7×10^{-3}	0.06	0.17	3.89	1.3×10^{-2}	0.06	21.2
5/12/78		0.24	6.44	6.4×10^{-3}	0.06	0.39	7.53	1.3×10^{-2}	0.06	15.2
5/30/78		0.17	5.25	6.8×10^{-3}	0.06	0.26	5.75	1.4×10^{-2}	0.06	30.1
5/01/78	R6	0.17	5.73	12.0×10^{-3}	0.06	0.27	6.37	2.5×10^{-2}	0.06	22.0
5/12/78		0.36	6.38	4.9×10^{-3}	0.06	0.56	7.21	0.9×10^{-2}	0.06	15.6
5/30/78		0.14	4.80	9.3×10^{-3}	0.06	0.22	5.27	2.0×10^{-2}	0.06	28.4
5/01/78	R7	0.29	4.92	13.9×10^{-3}	0.06	0.41	5 06	2.6×10^{-2}	0.06	19.6
5/12/78		0.18	3.43	6.5×10^{-3}	0.06	0.26	3.55	1.3×10^{-2}	0.06	12.7
5/30/78		0.35	6.17	21.2×10^{-3}	0.06	0.51	6.56	4.1×10^{-2}	0.06	19.9
5/01/78	R8	0.21	3.67	28.1×10^{-3}	0.06	0.31	3.95	5.9×10^{-2}	0.06	22.3
5/12/78		0.18	4.22	14.6×10^{-3}	0.06	0.26	4.44	2.9×10^{-2}	0 06	13.0
5/30/78		0.30	5.69	29.7×10^{-3}	0.06	0.44	6.06	5.8×10^{-2}	0.06	23.5

9164-83

In addition to the soil surface conditions and the vegetation parameters as discussed in the previous section, soil moisture content also has a large effect on the backscattering coefficient. Figure 6 demonstrates some of the calculated results of $\sigma^o(\theta)$ as a function of volumetric soil moisture (SM) at the five incidence angles of 10^o, 20^o, 30^o, 40^o, and 50^o, as labeled on the curves. These results for L- and C-band were calculated with the average values of the best-fit parameters, as given in the bottom row of Table 1.

Figure 6 shows that the backscattering coefficient increases with SM. Its increment in low SM region is faster than that at high SM (>30%). Below SM = 30%, the $\sigma^o(\theta)$ values in Figure 6 vary approximately linearly with SM. Linear regression analysis of $\sigma^o(\theta)$ values below SM = 30% was performed, and the results are listed in Table 3, which contains the values of intercept and slope for each incidence angle.

Table 3 shows that the backscattering coefficient sensitivity to soil moisture, defined as $d\sigma^o(\theta)/dSM$ (which equals to the slope of the regression line), decrease as the incidence angle θ increases. At $\theta > 40^o$, Table 3 shows the slope values are almost zero (i.e., $d\sigma^o(\theta)/dSM \approx 0$). This is due to the fact that the vegetation scattering is the primary contribution to the backscattering coefficient at large angles. The slope values in Table 3 are in good agreement with the results reported by Ulaby et al., [6].

Table 3 also shows that the slopes for both L- and C-band are relatively constant up to 20^o, but that the intercept changes by about 10 dB in L-band and 8 dB in C-band.

Figure 7 shows the comparison of the calculated backscattering coefficients and the scatterometer data at $\theta = 10^o$, as a function of volumetric soil moisture. The calculated results

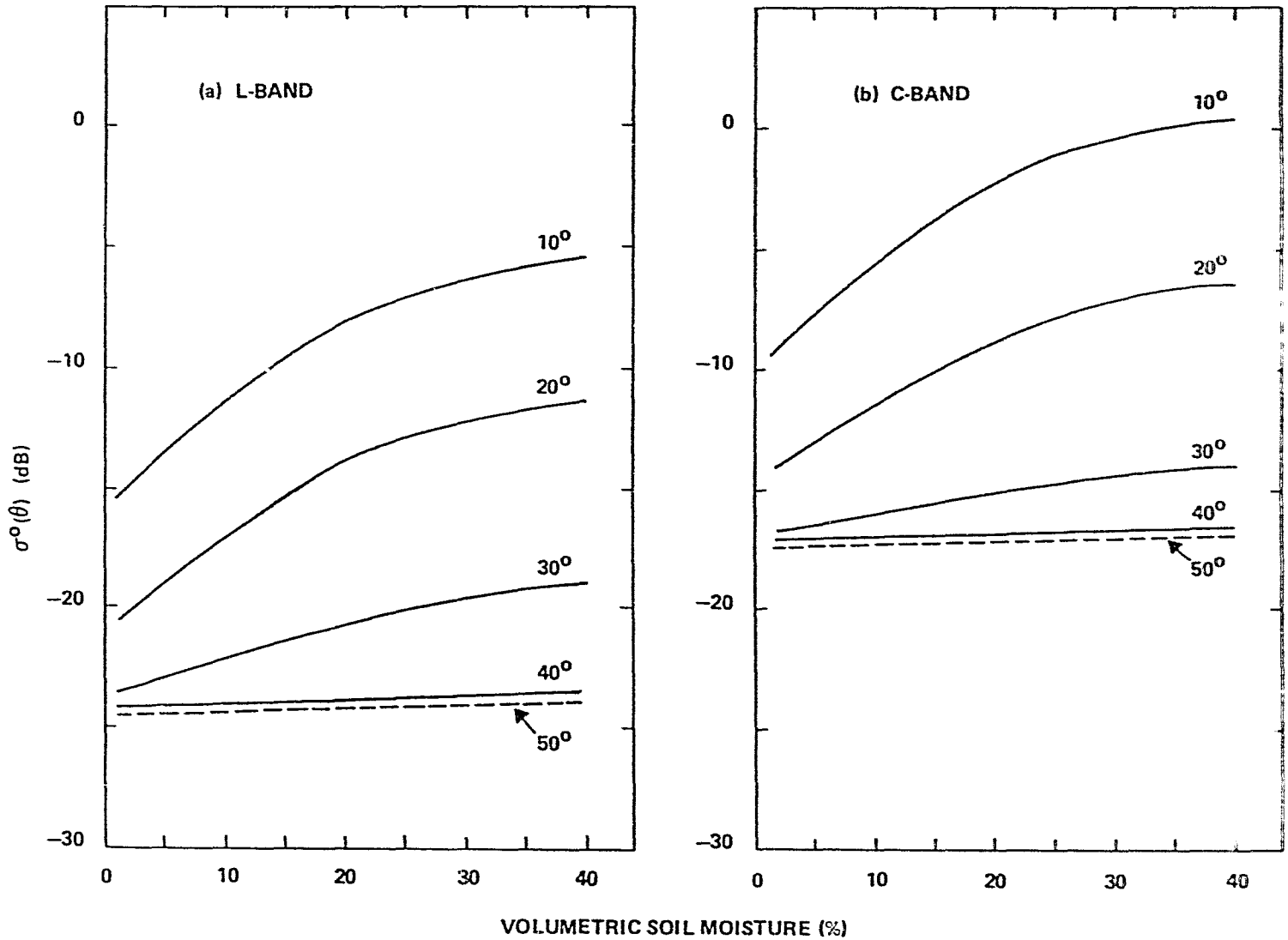

Figure 6. Backscattering coefficients (at fixed incidence angle) vesus volumetric soil moistures. These results were calculated using the average parameters as listed in the bottom row in Table 1,and the ground was assumed to have uniform profiles of soil moisture and a temperature of 293°K, (a) L-band (b) C-band.

Table 3. Linear regression results of backscattering coefficient versus volumetric soil moisture (<30%), at different incident angles θ.

θ (DEGREE)	L-BAND		C-BAND	
	INTERCEPT	SLOPE	INTERCEPT	SLOPE
5	−9.5	0.32	−6.5	0.32
10	−14.9	0.31	−9.5	0.31
15	−17.4	0.30	−12.0	0.28
20	−19.9	0.27	−14.6	0.24
25	−22.2	0.22	−16.4	0.16
30	−23.6	0.14	−17.2	0.07
35	−24.1	0.06	−17.4	0.03
40	−24.3	0.02	−17.4	0.01
45	−24.3	0.00	−17.5	0.00
50	−24.4	0.00	−17.6	0.00

9164-(50)-83

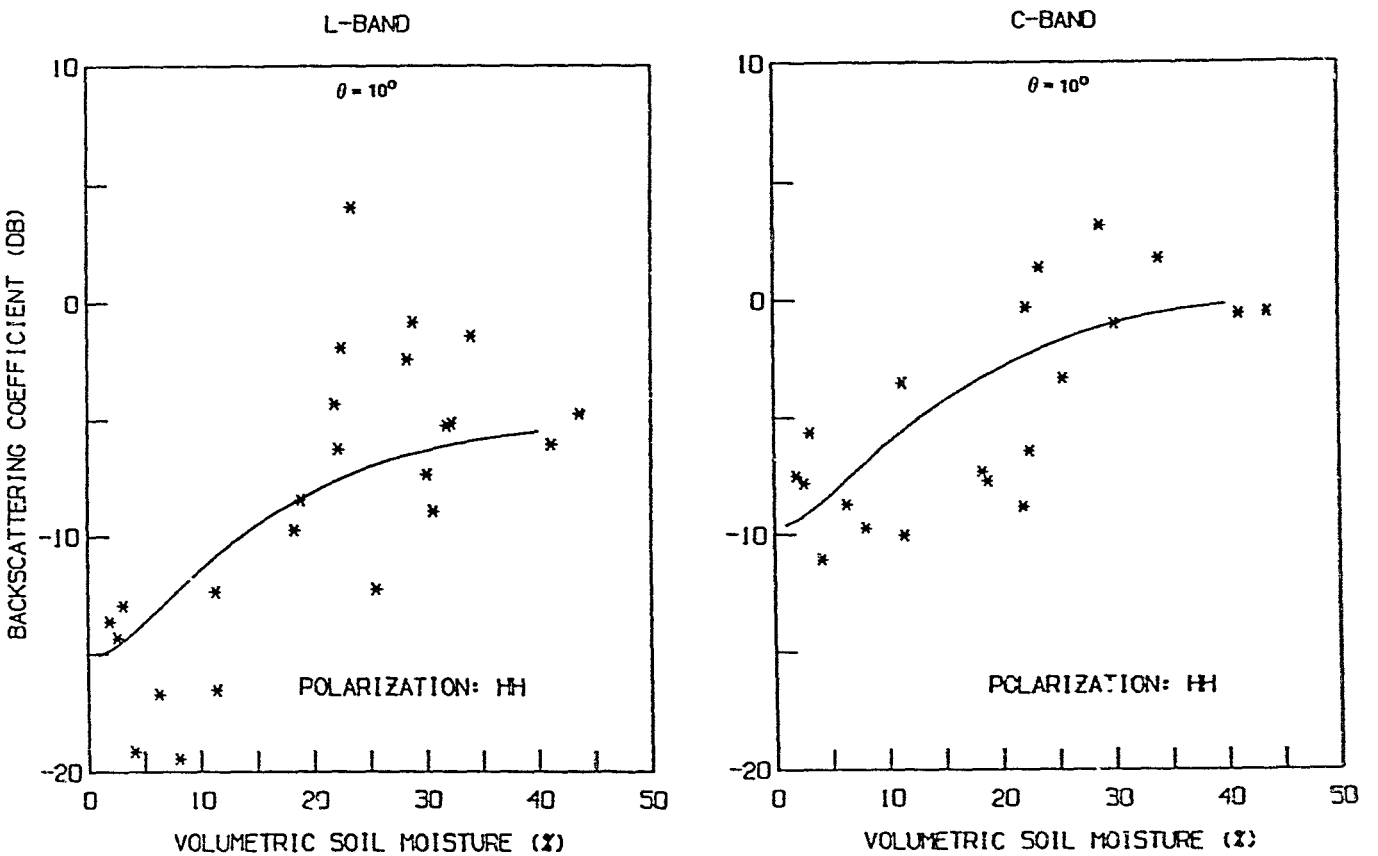

Figure 7. Comparison of calculated and measured backscattering coefficients at $\theta = 10^{o}$.

(solid curves) are the same as shown in Figure 6, and the data (asterisks) are plotted as a function of the soil moisture within the surface 0-2.5 cm of soil depth. Figure 7 demonstrates that the agreement between the calculations and data is reasonably good within experimental errors.

5. CONCLUSIONS

We have shown that the measured angular distribution of backscattering coefficient of vegetation-covered fields can be satisfactorily reproduced, using the model developed in this study. The model takes into consideration both coherent and incoherent scattering from rough soil surfaces. In addition, the vegetation scattering is also included in the model and it appears to be dominant at large incident angles (i.e., $\theta > 30^{\circ}$). The coherent scattering component, which is very important at angles near nadir, is introduced into the model through the antenna gain pattern with finite 3-dB beamwidth. The incoherent scattering, which vanishes for a smooth soil surface, contributes to the backscattering coefficient at all incident angles for rough soil surfaces.

The $k\sigma$ values obtained from best fits to scatterometer data of various sites qualitatively correlate with the degree of roughness of the soil surfaces. Also, the frequency-dependence of the best-fit $k\sigma$ values is in agreement with expectation in most cases (Table 1). This implies that by least-squares fit to the scatterometer data, one can obtain reliable value of the standard deviation of a rough surface. However, the $k\ell$ values do not scale properly with wavelength.

Acknowledgment: We would like to thank Drs. Bruce Blanchard and James Wang for discussions concerning the operations of the scatterometers.

APPENDIX A

This appendix presents additional calculations and comparisons of scatterometer data of backscattering coefficients for HH polarization over grass-covered fields as described in the main text of this study. It contains 20 measurements at L-band, and 16 measurements at C-band (only L-band measurements were taken on May 1, 1978).

Each set of calculated and observed results is plotted as a function of incidence angle. The parameters used in the calculations are listed at the top of each plot. These parameters are also listed in in Table 1. The asterisks (*) denote the scatterometer data, and the solid curves represented the calculated results. The figures (Figures A-1 through A-20) are arranged according to the field sites, and dates.

ORIGINAL PAGE IS
OF POOR QUALITY

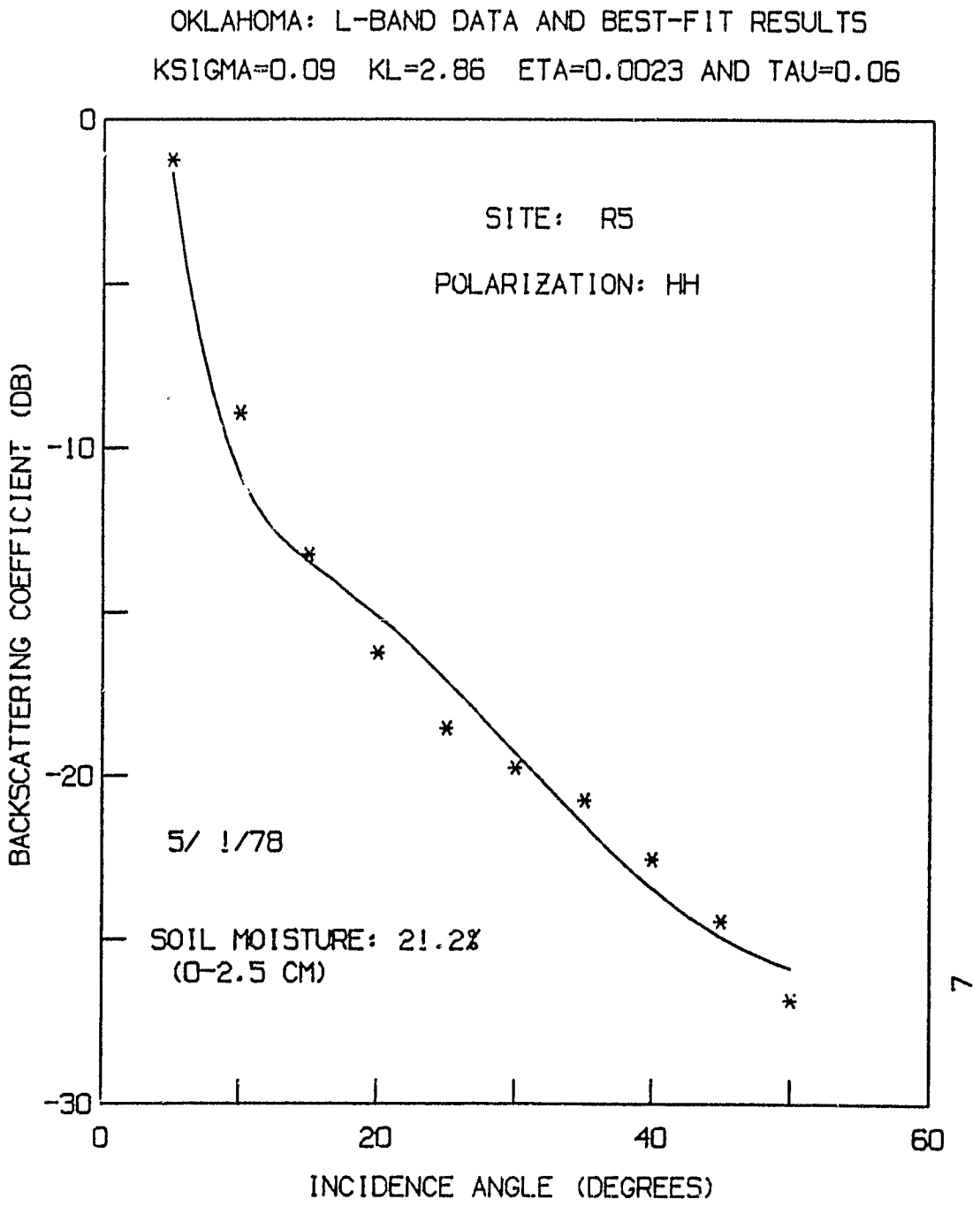

Figure A-1

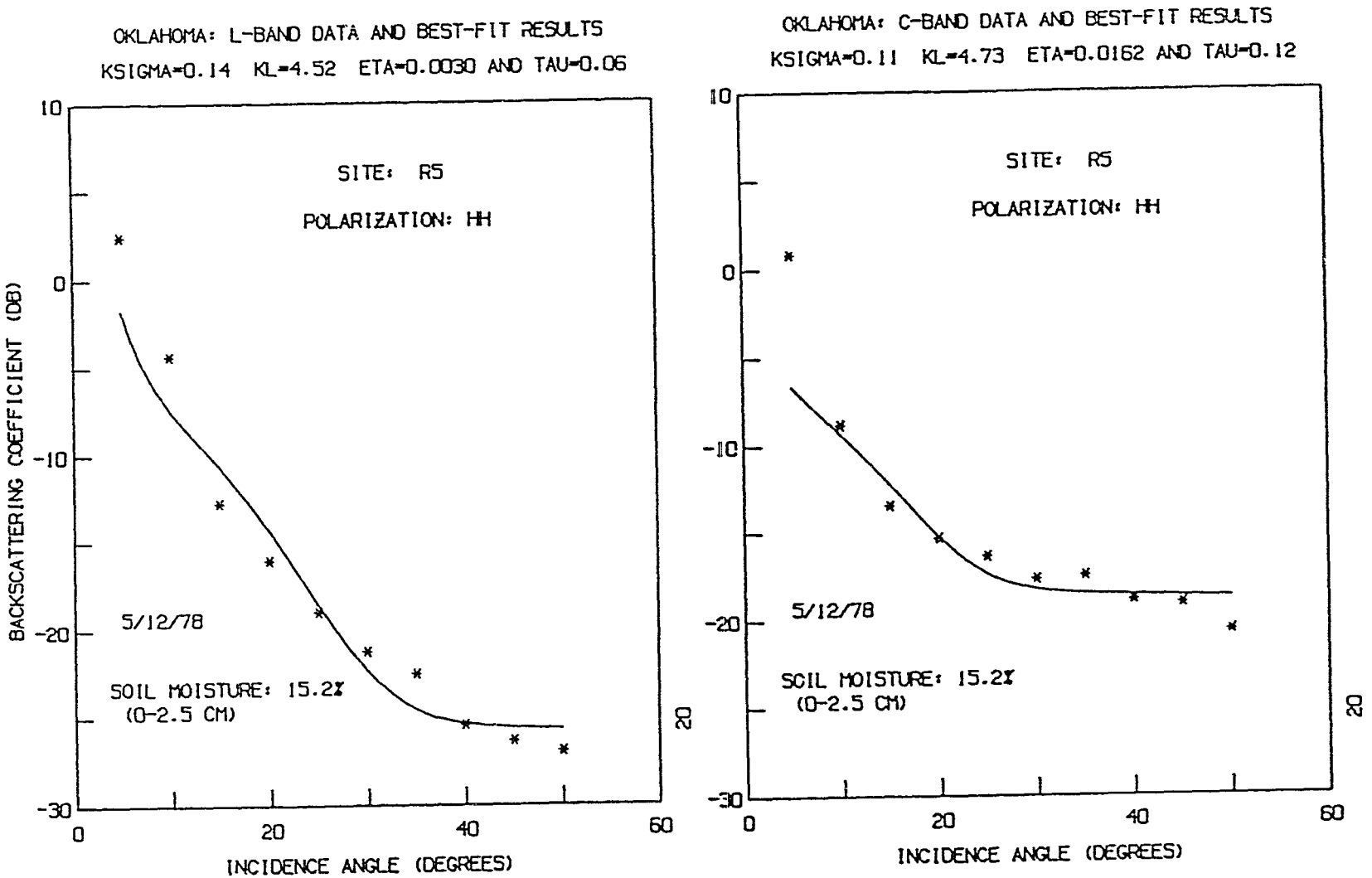

Figure A-2

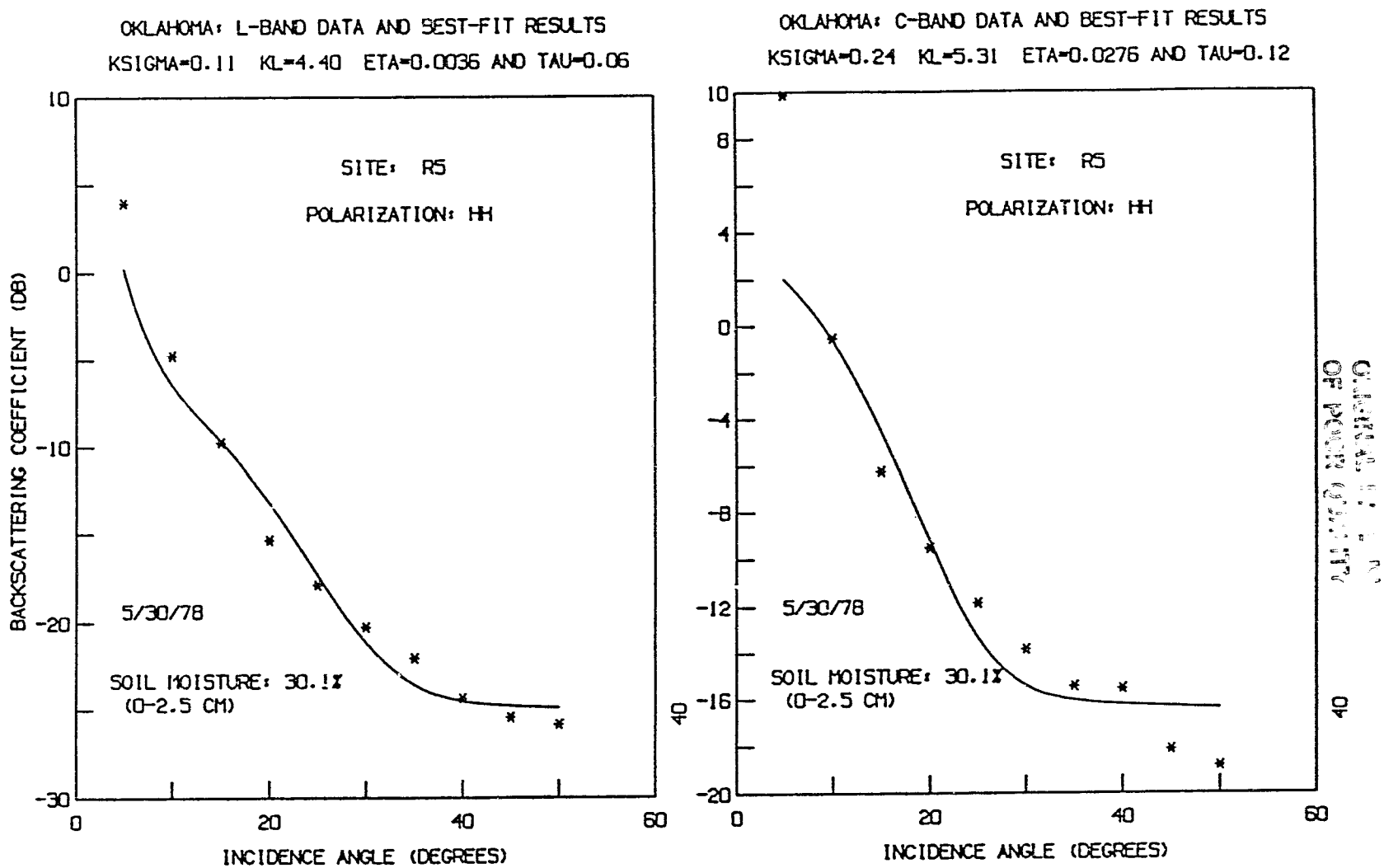
OKLAHOMA: L-BAND DATA AND BEST-FIT RESULTS
KSIGMA=0.11 KL=4.40 ETA=0.0036 AND TAU=0.06
SITE: R5
POLARIZATION: HH
5/30/78
SOIL MOISTURE: 30.1%
(0-2.5 CM)
BACKSCATTERING COEFFICIENT (DB)
INCIDENCE ANGLE (DEGREES)
OKLAHOMA: C-BAND DATA AND BEST-FIT RESULTS
KSIGMA=0.24 KL=5.31 ETA=0.0276 AND TAU=0.12
SITE: R5
POLARIZATION: HH
5/30/78
SOIL MOISTURE: 30.1%
(0-2.5 CM)
INCIDENCE ANGLE (DEGREES)

Figure A-3

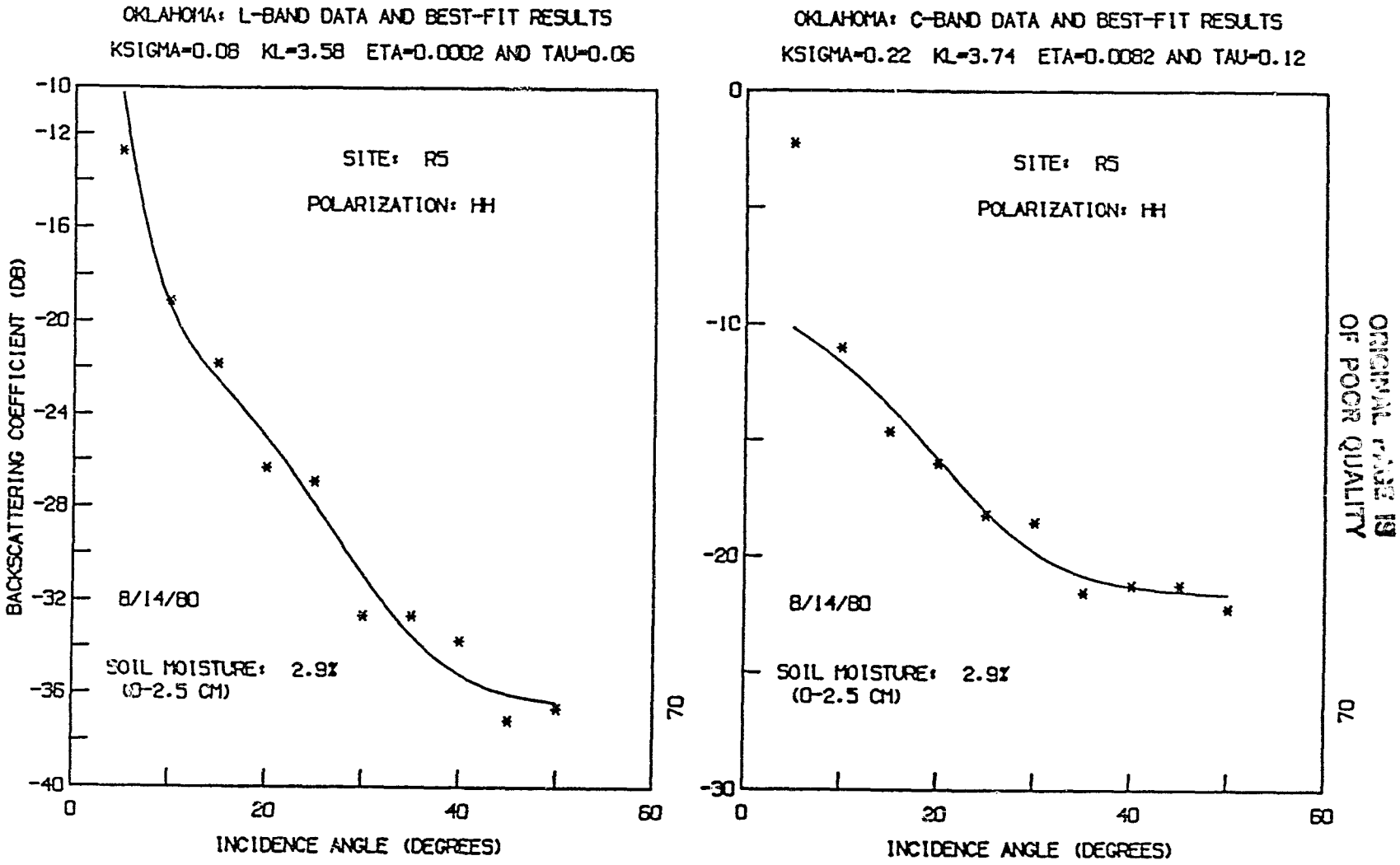
OKLAHOMA: L-BAND DATA AND BEST-FIT RESULTS
KSIGMA=0.08 KL=3.58 ETA=0.0002 AND TAU=0.06
SITE: R5
POLARIZATION: HH
8/14/80
SOIL MOISTURE: 2.9%
(0-2.5 CM)
BACKSCATTERING COEFFICIENT (DB)
INCIDENCE ANGLE (DEGREES)
OKLAHOMA: C-BAND DATA AND BEST-FIT RESULTS
KSIGMA=0.22 KL=3.74 ETA=0.0082 AND TAU=0.12
SITE: R5
POLARIZATION: HH
8/14/80
SOIL MOISTURE: 2.9%
(0-2.5 CM)
INCIDENCE ANGLE (DEGREES)

Figure A-4

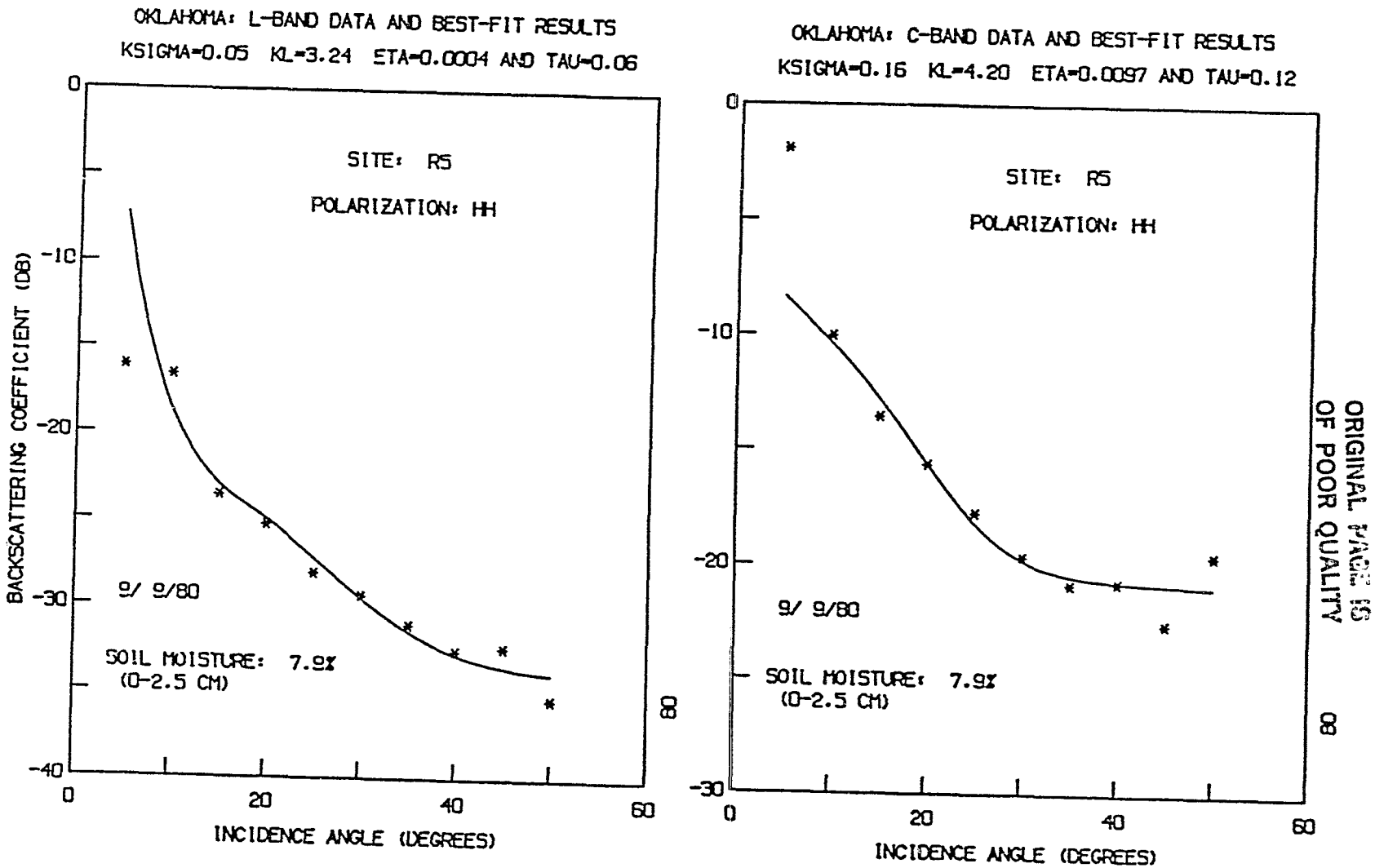

Figure A-5

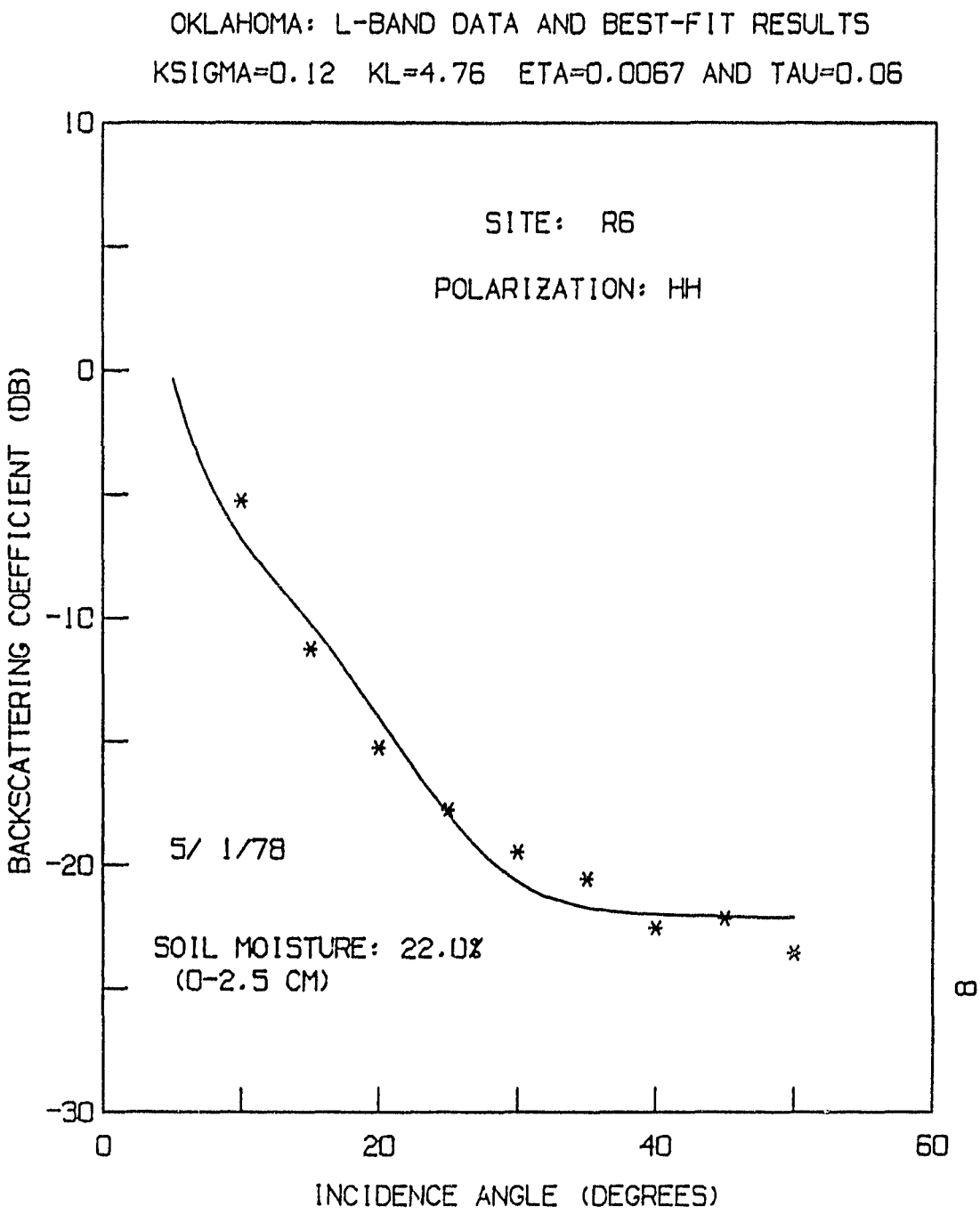

Figure A-6

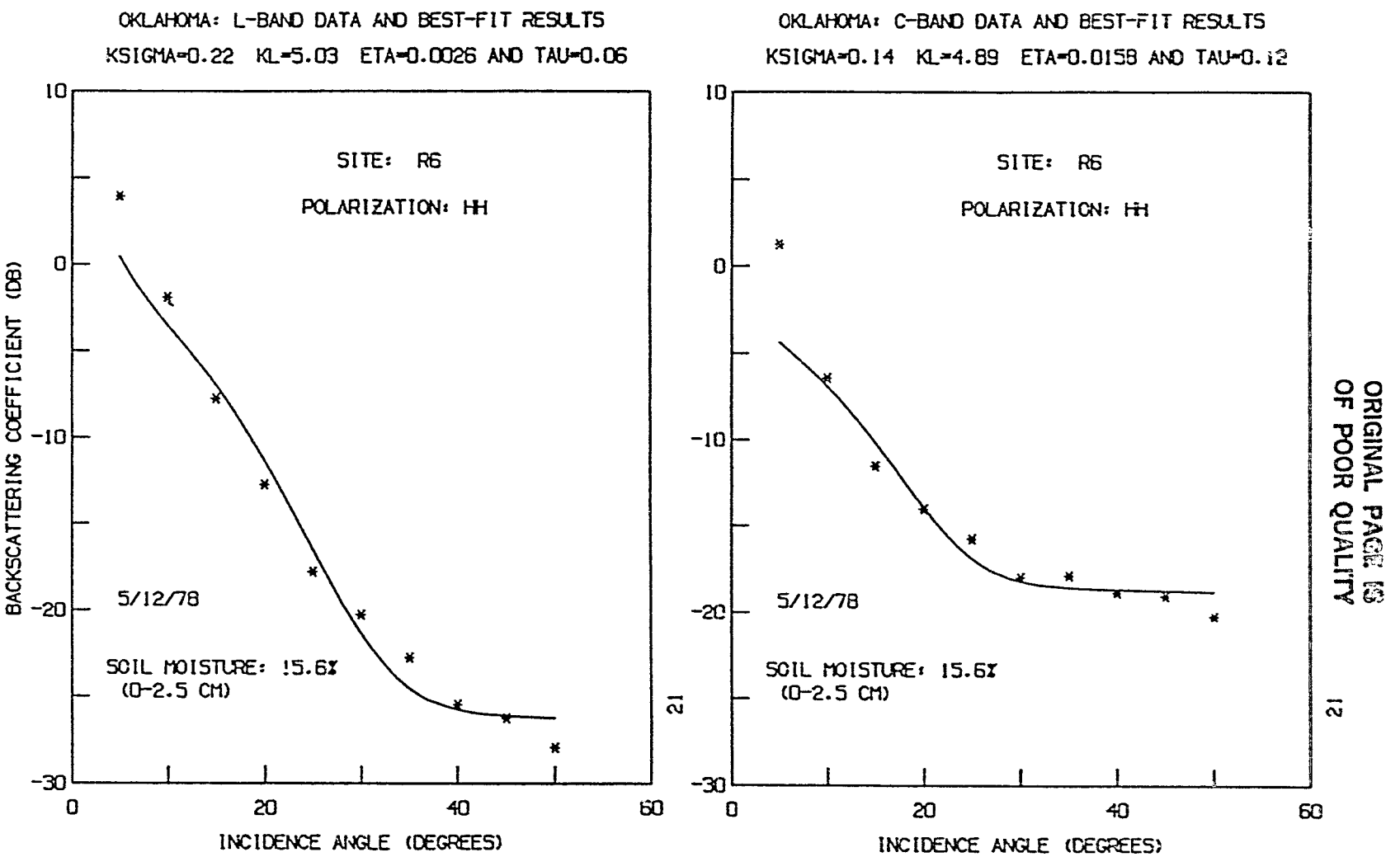

Figure A-7

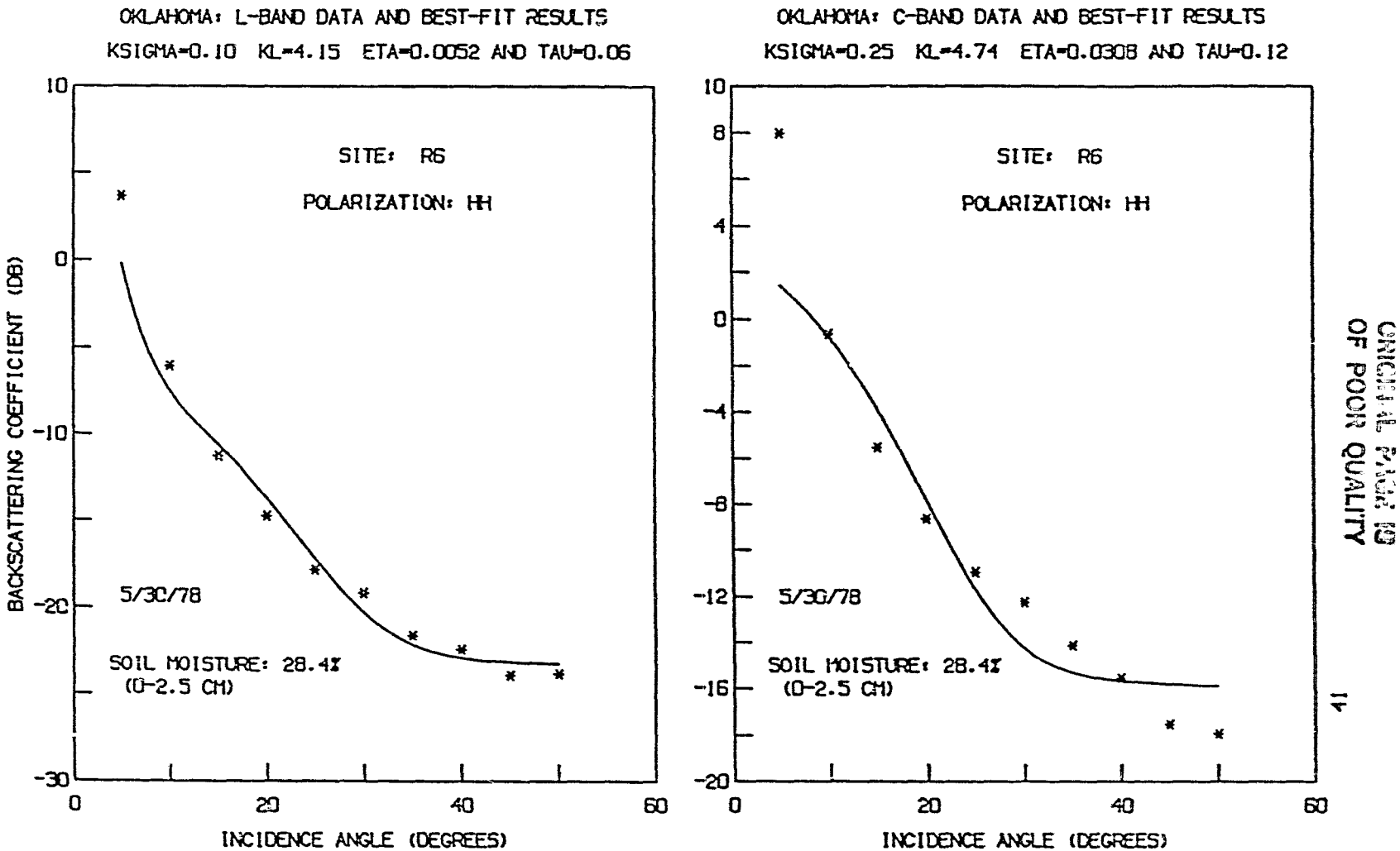
OKLAHOMA: L-BAND DATA AND BEST-FIT RESULTS
KSIGMA=0.10 KL=4.15 ETA=0.0052 AND TAU=0.06
SITE: R6
POLARIZATION: HH
5/30/78
SOIL MOISTURE: 28.4%
(0-2.5 CM)
BACKSCATTERING COEFFICIENT (DB)
INCIDENCE ANGLE (DEGREES)
OKLAHOMA: C-BAND DATA AND BEST-FIT RESULTS
KSIGMA=0.25 KL=4.74 ETA=0.0308 AND TAU=0.12
SITE: R6
POLARIZATION: HH
5/30/78
SOIL MOISTURE: 28.4%
(0-2.5 CM)
INCIDENCE ANGLE (DEGREES)

Figure A-8

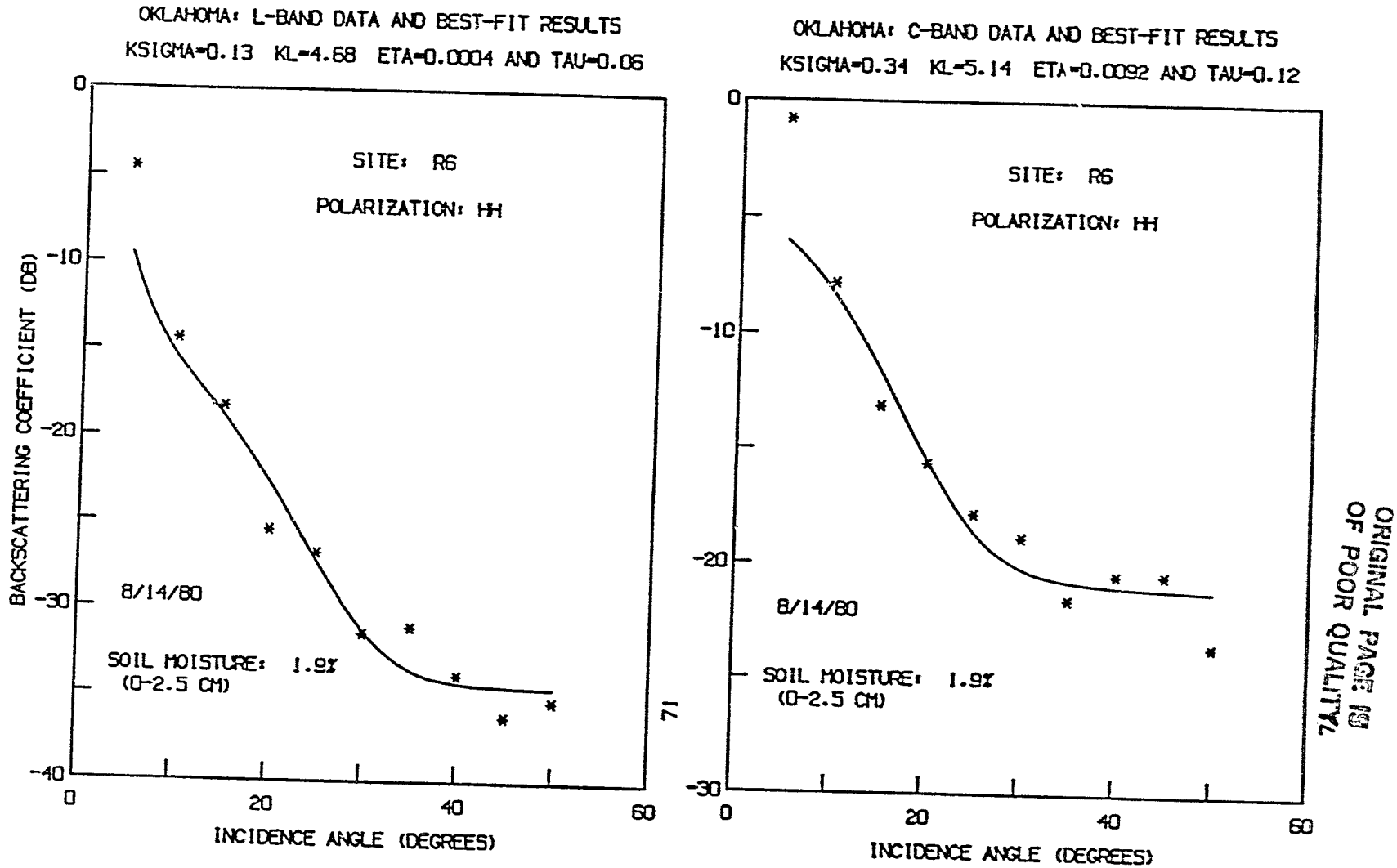

Figure A-9

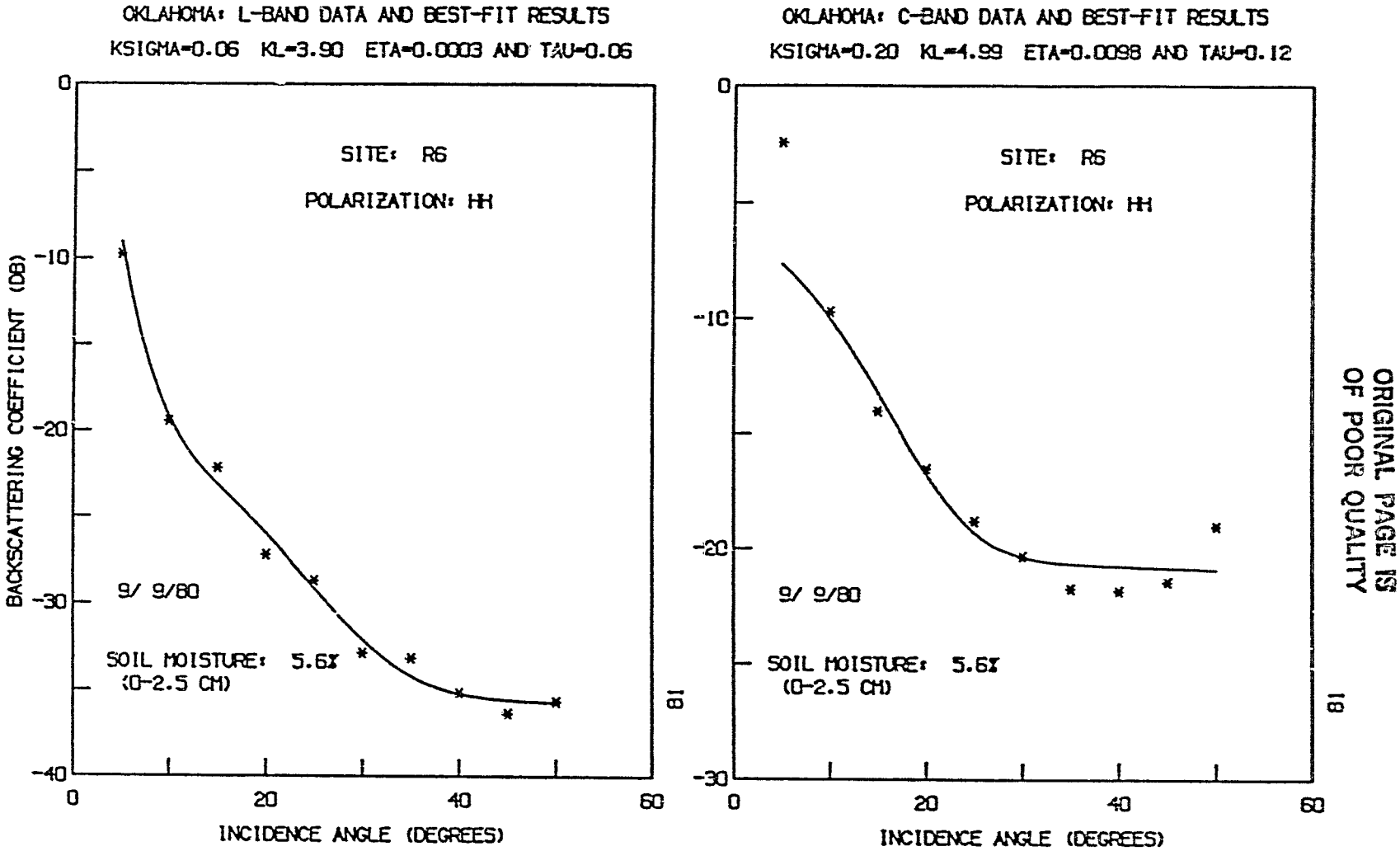

Figure A-10

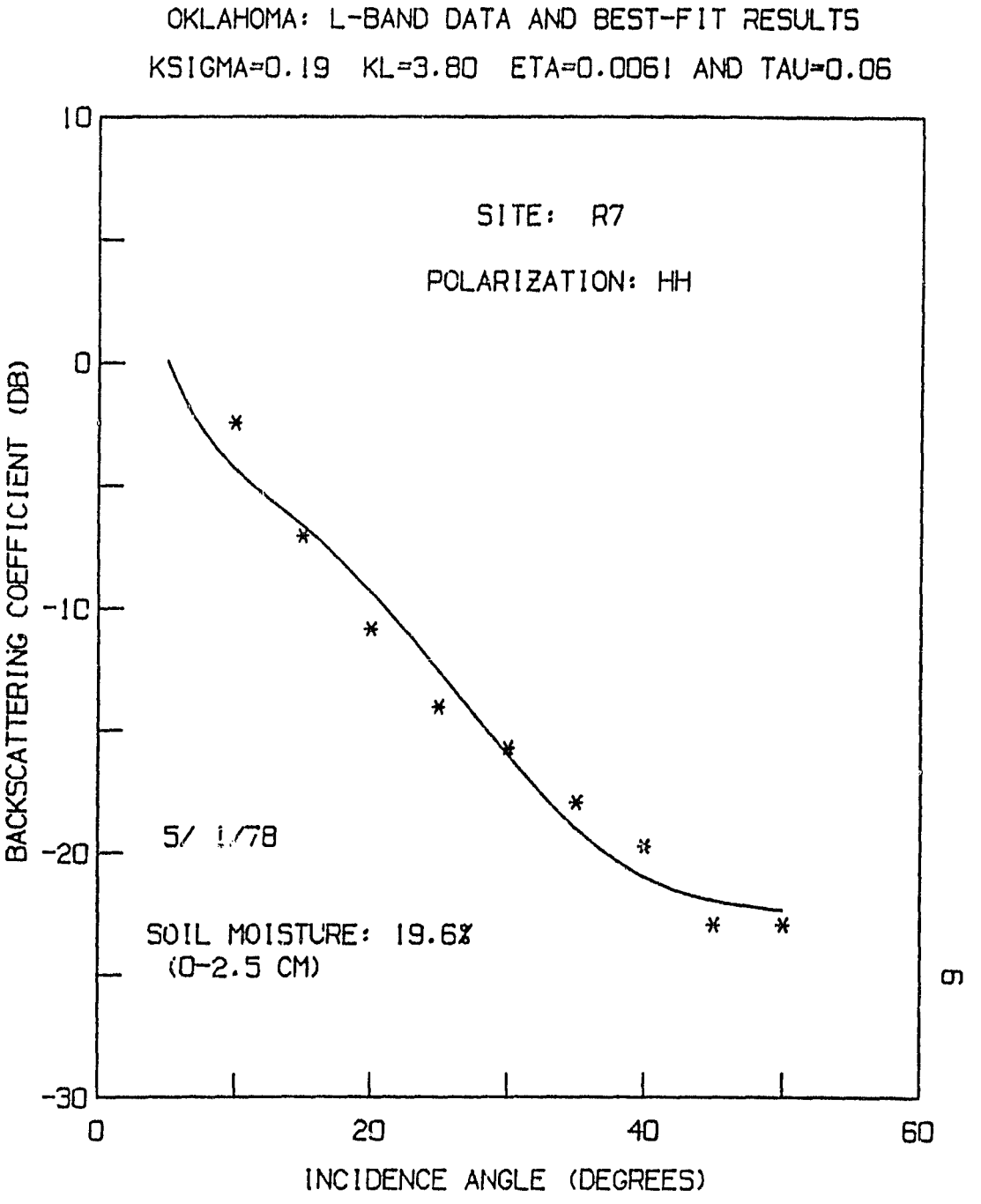

Figure A-11

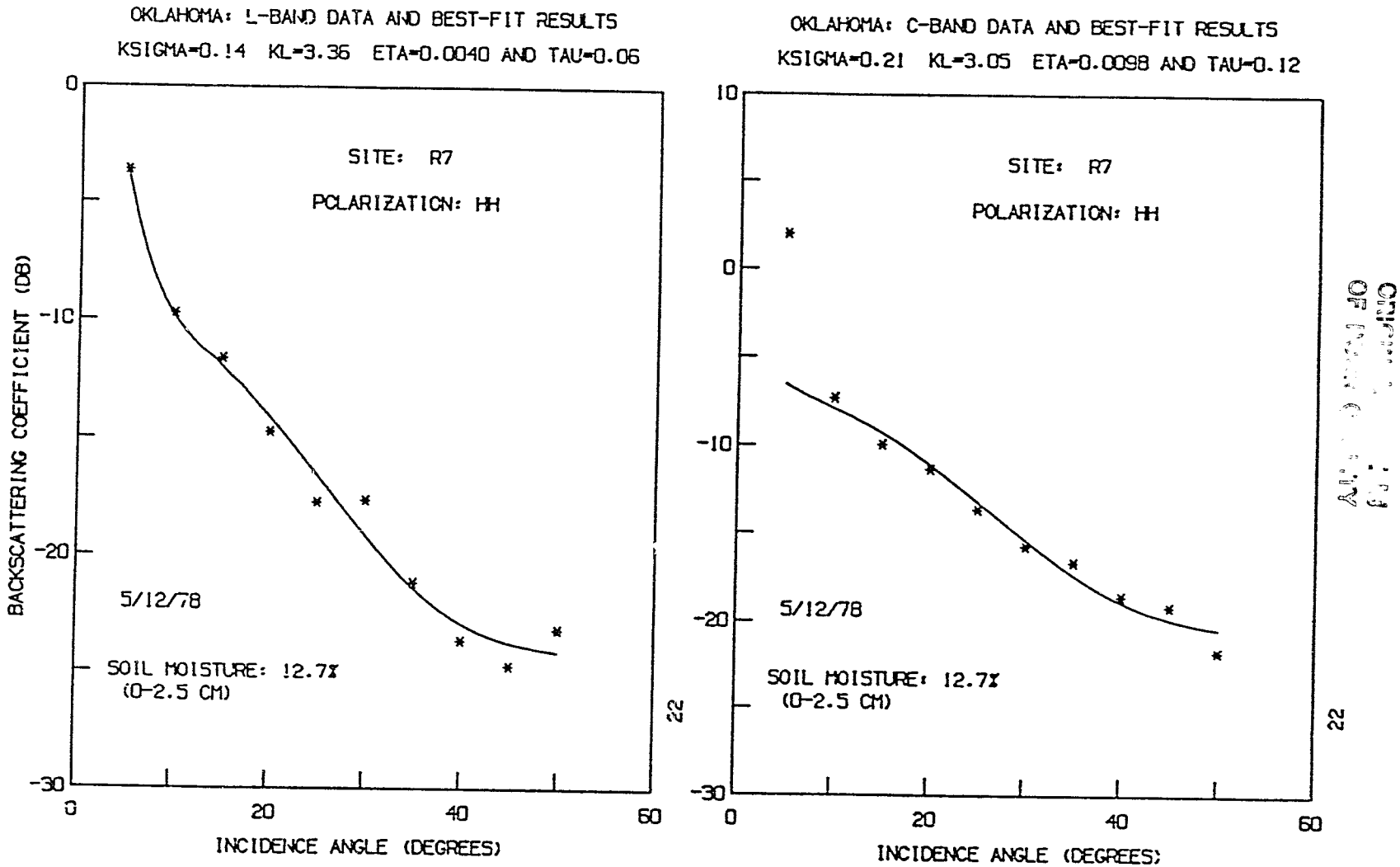
OKLAHOMA: L-BAND DATA AND BEST-FIT RESULTS
KSIGMA=0.14 KL=3.36 ETA=0.0040 AND TAU=0.06
SITE: R7
POLARIZATION: HH
5/12/78
SOIL MOISTURE: 12.7%
(0-2.5 CM)
BACKSCATTERING COEFFICIENT (DB)
INCIDENCE ANGLE (DEGREES)
0
-10
-20
-30
0
20
40
60
OKLAHOMA: C-BAND DATA AND BEST-FIT RESULTS
KSIGMA=0.21 KL=3.05 ETA=0.0098 AND TAU=0.12
SITE: R7
POLARIZATION: HH
5/12/78
SOIL MOISTURE: 12.7%
(0-2.5 CM)
INCIDENCE ANGLE (DEGREES)
10
0
-10
-20
-30
0
20
40
60

Figure A-12

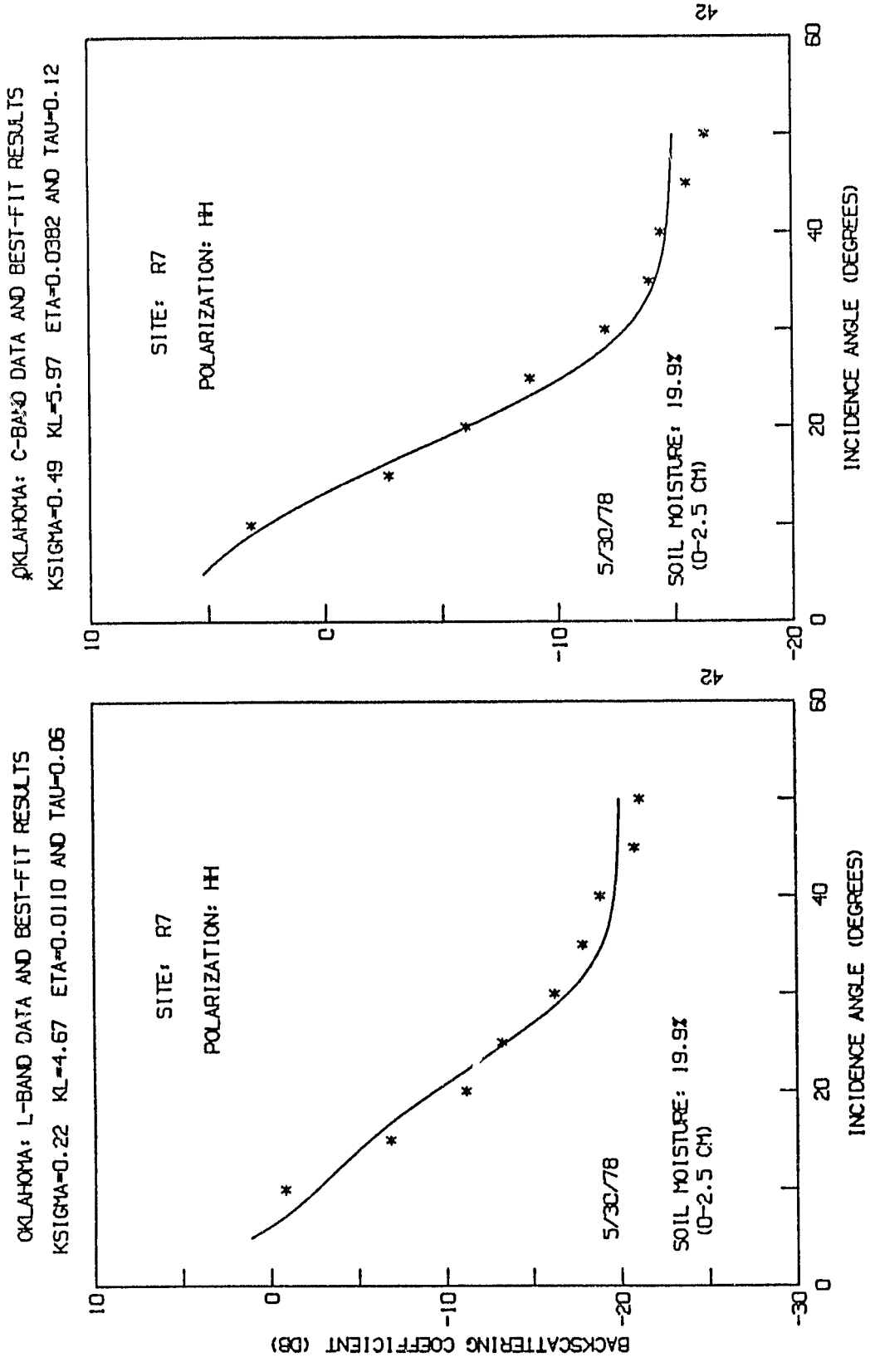

Figure A-13

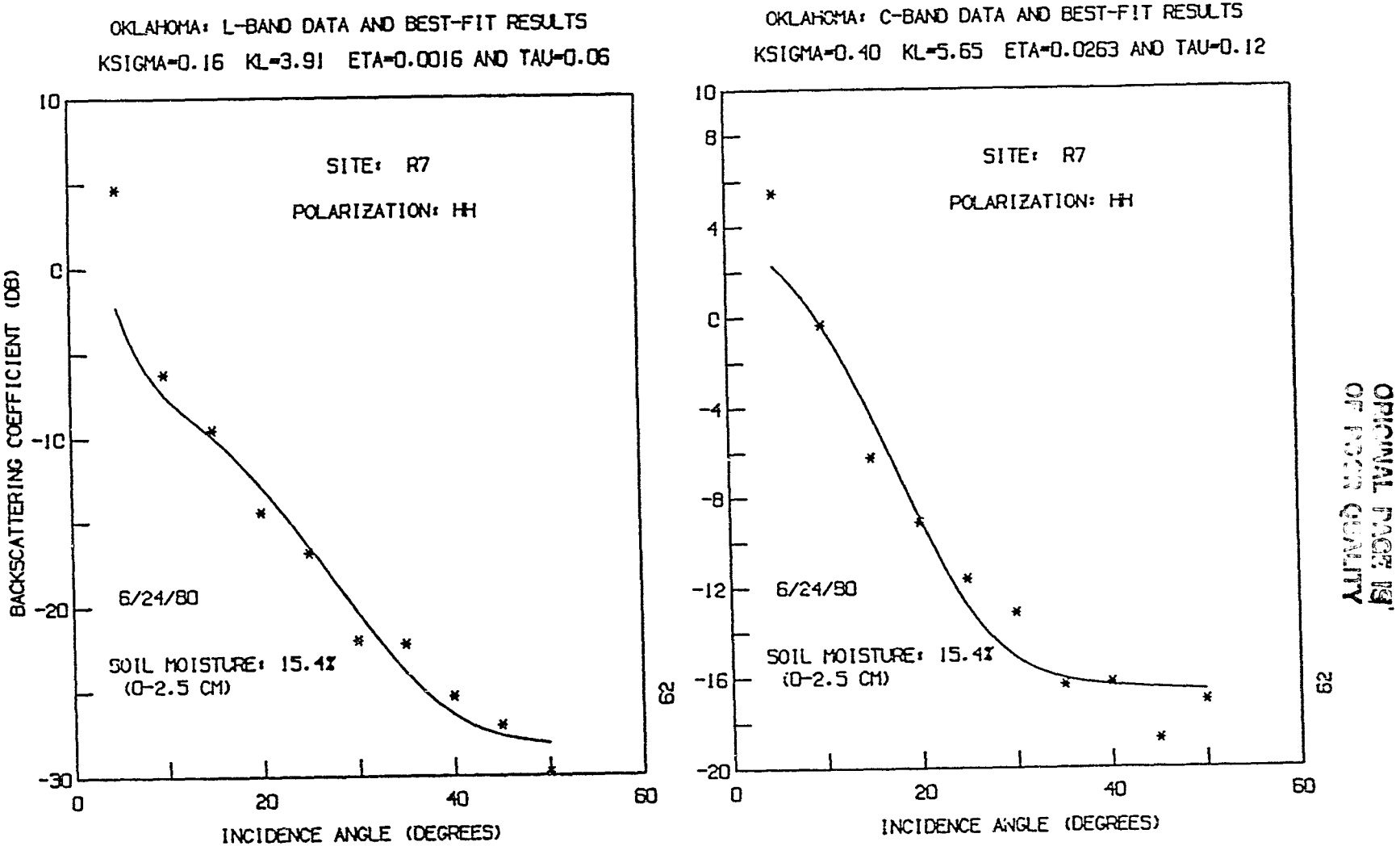

Figure A-14

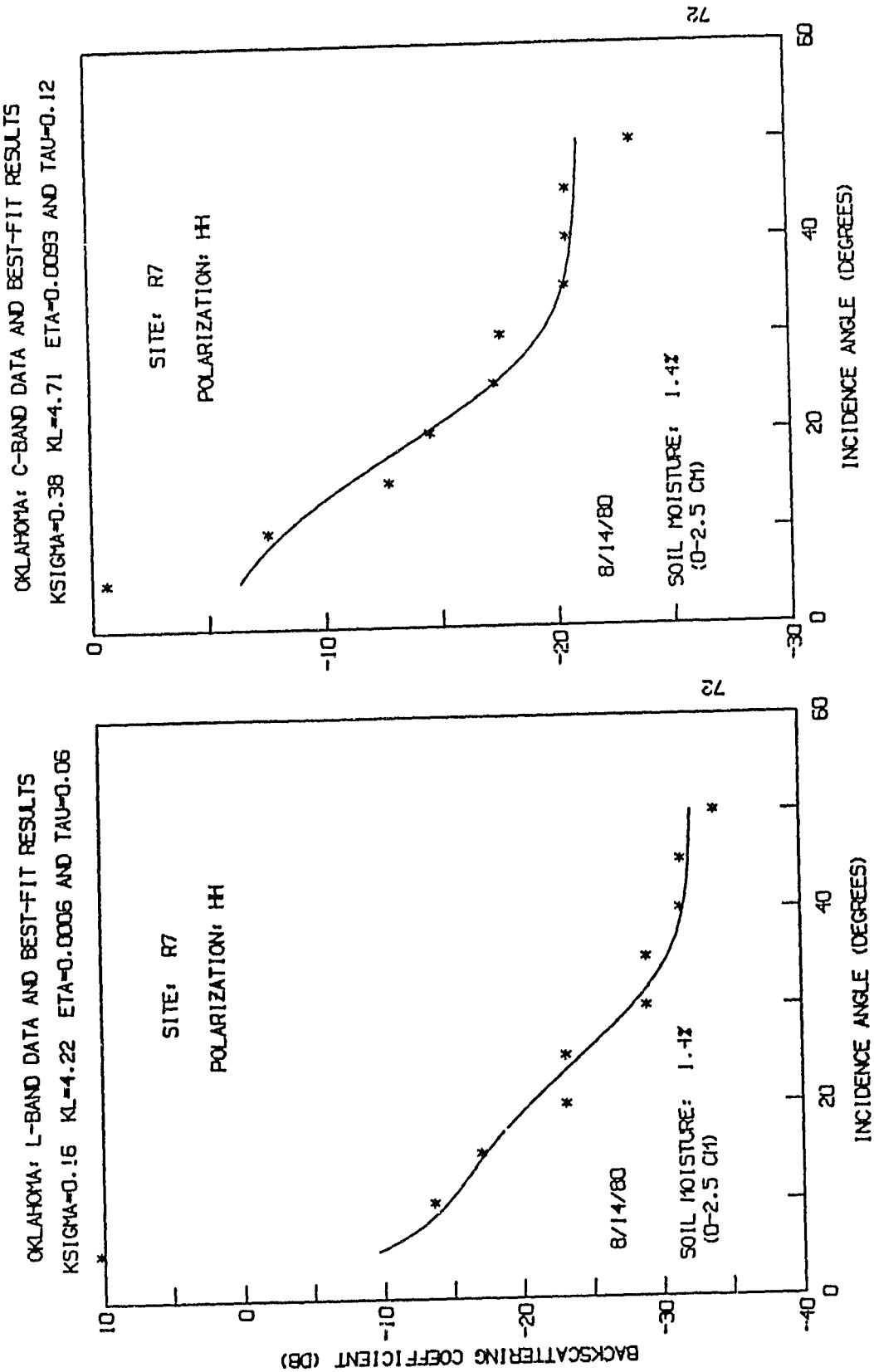

Figure A-15

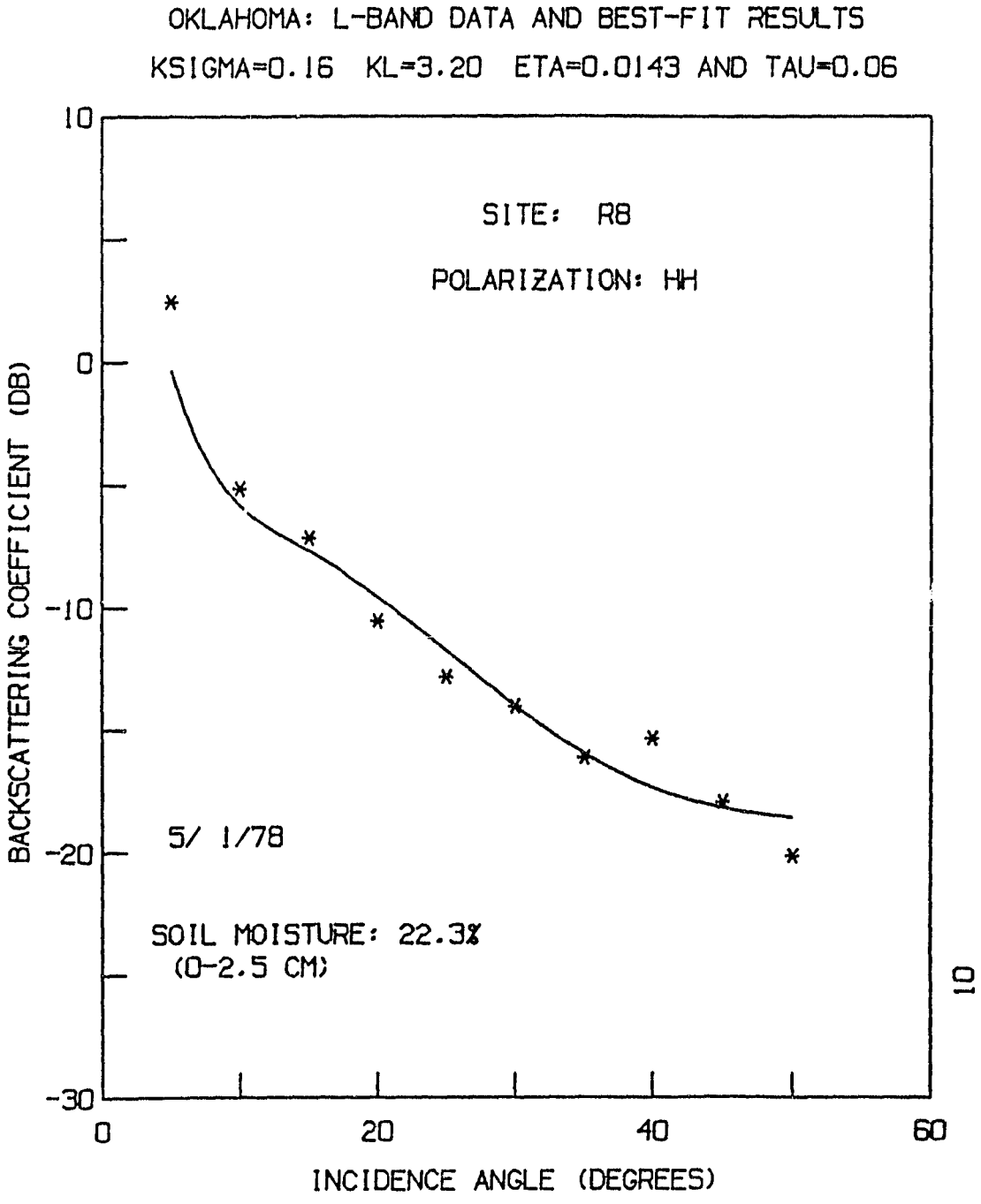

Figure A-16

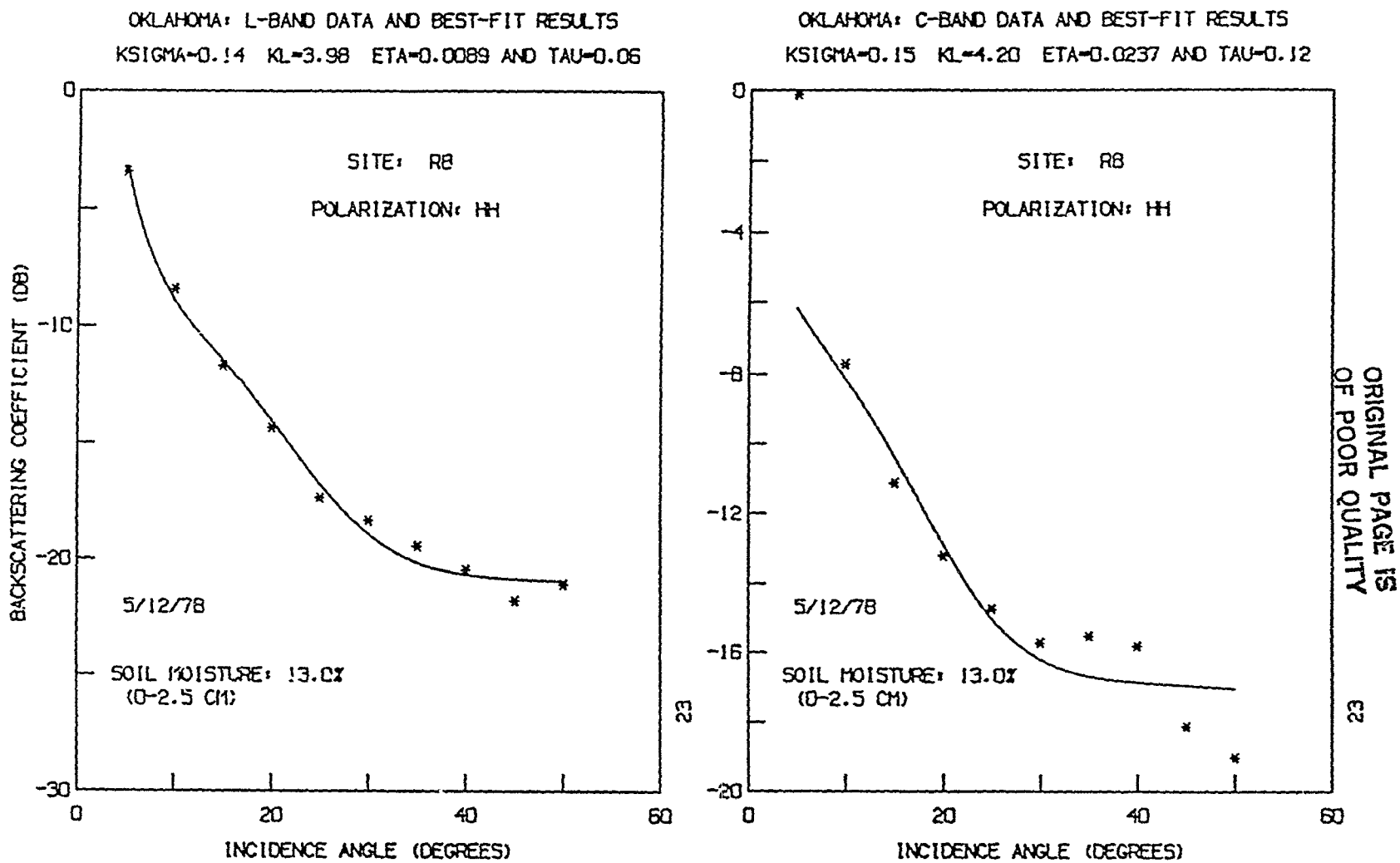

ORIGINAL PAGE IS
OF POOR QUALITY

Figure A-17

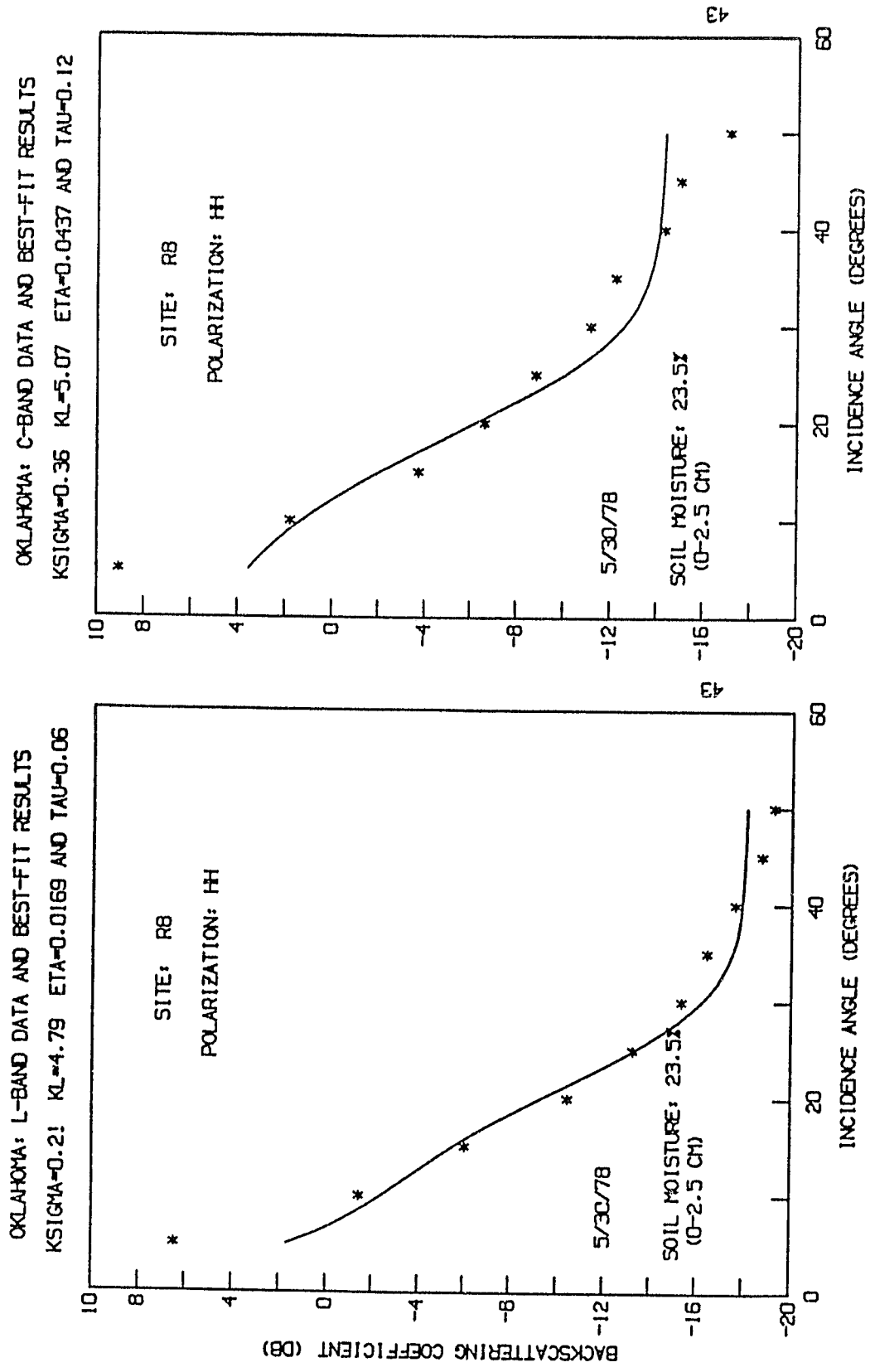

Figure A-18

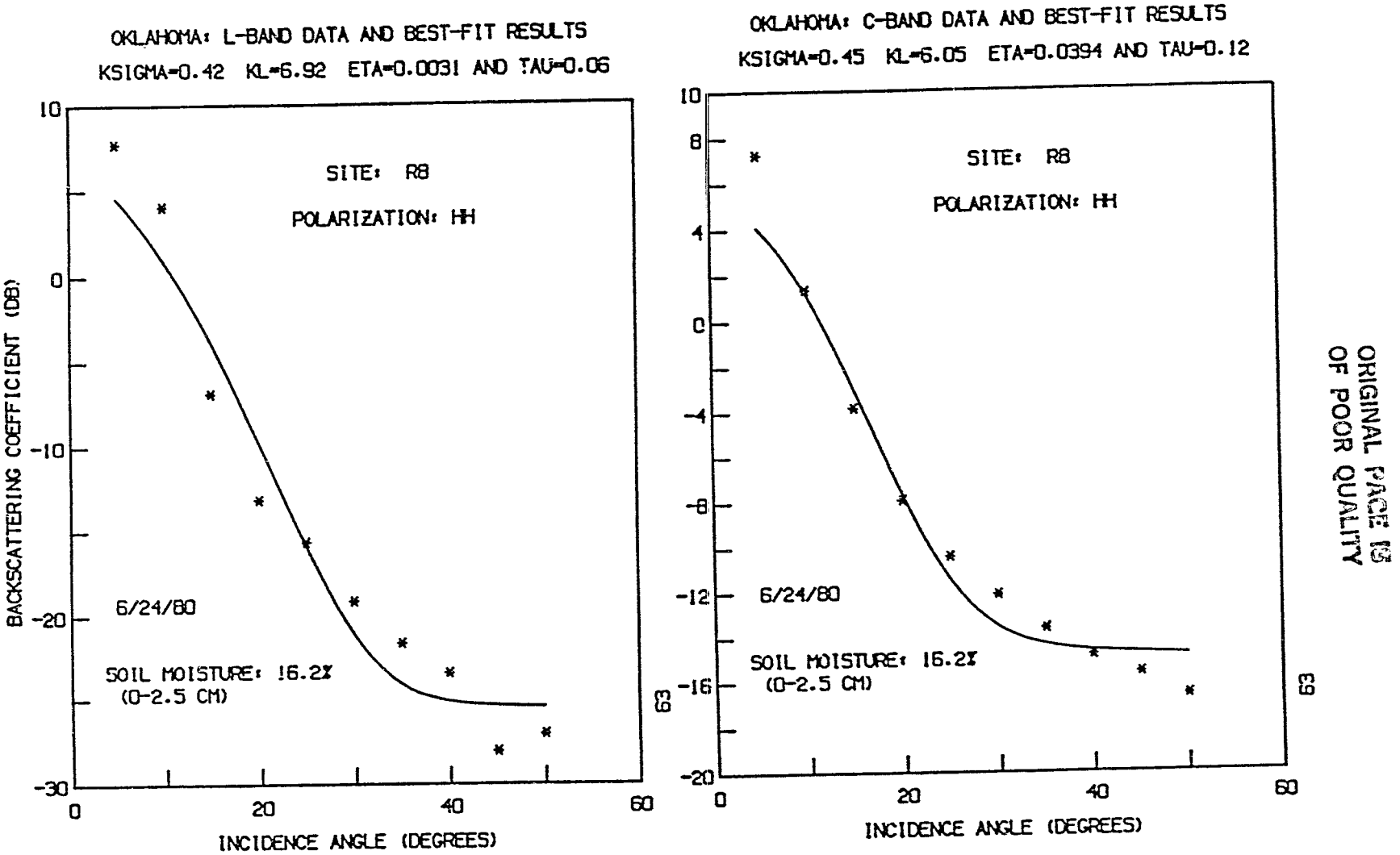

Figure A-19

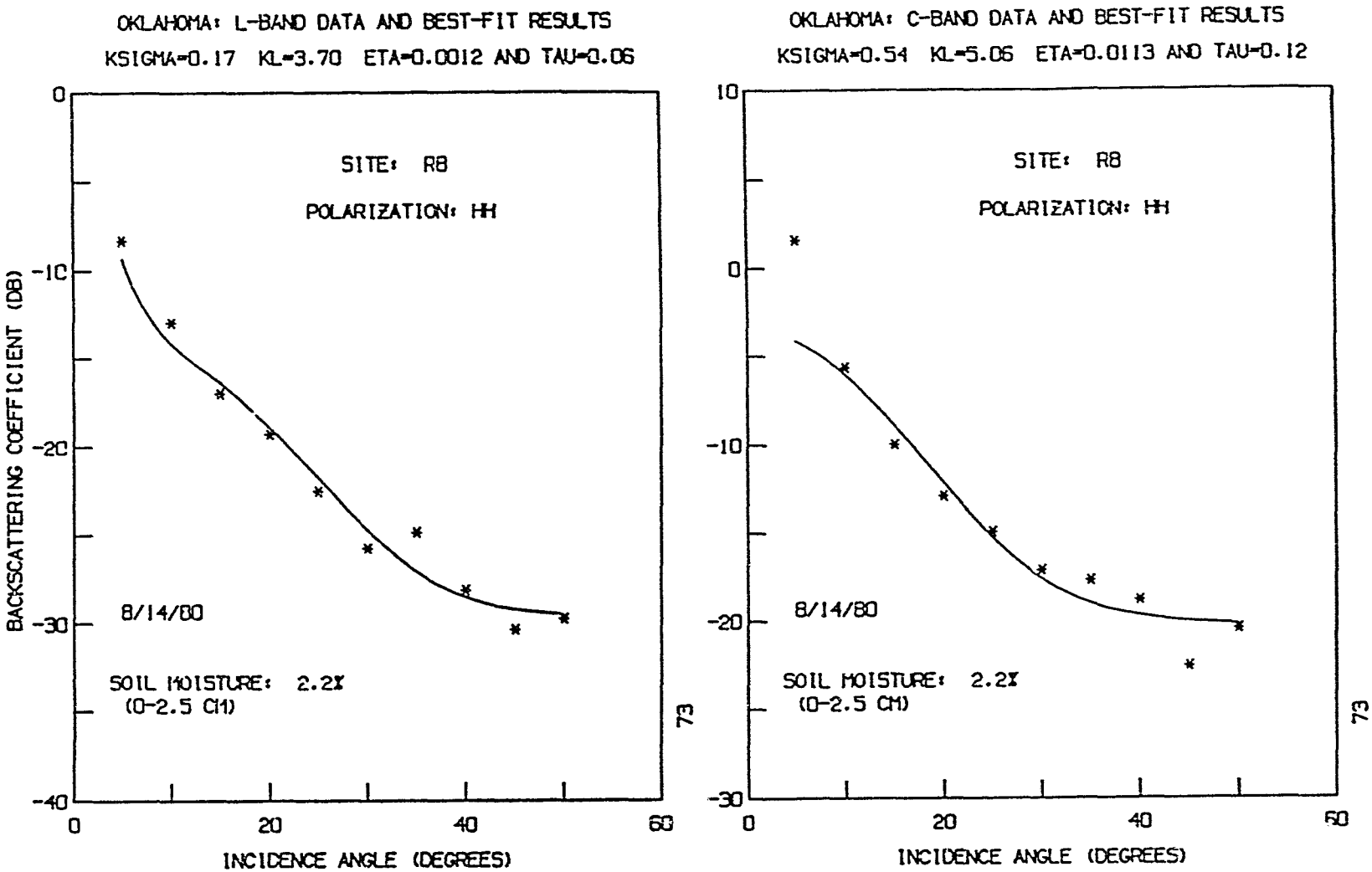

Figure A-20

REFERENCES

[1] Jackson, T. J., T. J. Schmugge, G. C., Coleman, C. Richardson, A. Chang, J. Wang, and E. T. Engman, "Aircraft Remote Sensing of Soil Moisture and Hydrologic Parameters, Chickasha, Okla., and Riesel, Tex., 1978 Data Report," ARR-NE-8, USDA, 1980

[2] Jackson, T. J., P. O'Neill, G. C. Coleman, T. J. Schmugge, "Aircraft Remote Sensing of Soil Moisture and Hydrologic Parameters, Chickasha, Okla., 1980 Data Report," USDA, 1982

[3] Theis, S. W., M. J. McFarland, W. D. Rosenthal, and C. L. Jones, "Microwave Remote Sensing of Soil Moistures," Technical Report RSC-3458-129, Remote Sensing Center, Texas A&M University, 1982

[4] Theis, S. W., M. J. McFarland, W. D. Rosenthal, and C. L. Jones, "Measurement of Soil Moisture Trends With Airborne Scatterometers," Technical Report RSC-3458-131, Remote Sensing Center, Texas A&M University, 1982

[5] Ulaby, F T., P. P. Batlivala, and M. C. Dobson, "Microwave Backscatter Dependence on Surface Roughness, Soil Moisture and Soil Texture: Part I - Bare Soil," IEEE Transactions on Geoscience Electronics, Vol. GE-16, pp. 286-295, 1978

[6] Ulaby, F. T., G. A. Bradley, and M. C. Dobson, "Microwave Backscatter Dependence on Surface Roughness, Soil Moisture and Soil Texture: Part II - Vegetation Covered Soil," IEEE Transactions on Geoscience Electronics, Vol. GE-19, pp. 33-40, 1981

[7] Allen, C. T., F. T. Ulaby and A. F. Fung, "A Model for the Radar Backscattering Coefficient of Bare Soil," University of Kansas Center for Research, Inc., Lawrence, KS, RSL TR 460-8 (AgRISTARS SM-K1-04181), 1982

[8] Attema, E. P. W. and F. T. Ulaby, "Vegetation Modeled as a Water Cloud," Radio Sci. vol. 13, no. 2, pp. 357-364, Mar-Apr., 1978

[9] Tsang, L., A. J. Blanchard, R. W. Newton, and J. A. Kong, "A Simple Relation Between Active and Passive Microwave Remote Sensing Measurements of Earth Terrain," IEEE Trans. Geosci. and Remote Sensing, GE-20, pp. 482-485, 1982

[10] Stogryn, A., "Electromagnetic Scattering From Rough Finitely Conducting Surfaces," Radio Sci. vol. 2, pp. 415-428, 1967

[11] Fung, A. K. and H. J. Eom, "An Approximate Model for Backscattering and Emission from Land and Sea" paper presented at the International Geoscience and Remote Sensing Symposium, IEEE Geosci. and Remote Sensing Soc., Washington, D.C., June 1981 (also TR SM-K1-0409, Remote Sensing Lab., University of Kansas)

[12] Fung, A. K. and H. J. Eom, "Note on the Kirchhoff Rough Surface Solution in Backscattering," Radio Sci., 16, pp. 299-302, 1981

[13] Semyonov, B., "Approximate Computation of Scattering of Electromagnetic Waves by Rough Surface Contours," Radio Engineering and Electronic Phys., Volume 11, pp., 1179-1187, 1966

[14] Ulaby, F. T., R. K. Moore and A. K. Fung, Microwave Remote Sensing: Active and Passive, vol. 2, Addison-Wesley Publishing Company, Reading, Massachusetts, 1982

[15] Wilheit, T. T. "Radiative Transfer in a Plane Stratified Dielectric," IEEE Trans. Geoscience Electron.," GE-16, pp. 138-143, 1978

[16] Mo, T., "Incoherent Scattering of Microwave Radiation From Rough Soil Surfaces," Computer Sciences Corporation, Silver Spring, MD CSC/TR-82/6001 (AgRISTARS SM-G2-04291), 1982

[17] Tsang, L., and R. W. Newton, "Microwave Emission from Soils with Rough Surfaces," J. Geophys, Res. vol. 11, pp. 9017-9024, 1982

[18] Jackson, T. J., "Preliminary Analysis of Aircraft Radar Data Collected at Chickasha, Oklahoma, 1978-1980," USDA Hydrology Laboratory, Beltsville, MD, Technical Report, 1983

[19] Wang, J. R., "A Model of the 1.6 GHz Scatterometer," Lockheed Electronics Company, Houston, TX, Job Order 75-415 (NASA/Johnson Space Center JSC-12990), 1977

[20] Blanchard, B. Personal Communication, 1983

[21] Mo. T., B. J. Choudhury, T. J. Schmugge, J. R. Wang and T. J. Jackson, "A Model for Microwave Emission From Vegetation-Covered Fields," J. Geophys. Res., 87, pp. 11229-11237, 1982

[22] Wang, J. R., J. Shiue, E. Engman, J. McMurtrey, P. Lawless, T. Schmugge, T. Jackson, W, Gould, J. Fuchs, C. Calhoon, T. Carnahan, E. Hirschmann, and W. Glazar. Remote Measurements of Soil Moisture by Microwave Radiometers at BARC Test Site, NASA Tech. Memo. 80720, 1980

[23] Eom, H. J., and A. K. Fung, "Scattering Coefficients of Kirchhoff Surfaces With Gaussian and non-Gaussian Surface Statistics," University of Kansas Center for Research, Inc., Lawrence, KS, RSL TR 4601-2 (AgRISTARS SM-K2-04370), 1982